Mathematical Modelling of Molecular Pathways Enabling Tumour Cell Invasion and Migration

David P A Cohen, Loredana Martignetti, Sylvie Robine, Emmanuel Barillot, Andrei Zinovyev, Laurence Calzone

▶ To cite this version:

HAL Id: inserm-02141625

https://inserm.hal.science/inserm-02141625

Submitted on 28 May 2019

Mathematical Modelling of Molecular Pathways Enabling Tumour Cell Invasion and Migration

David P. A. Cohen[1,2,3]**, Loredana Martignetti**[1,2,3]**, Sylvie Robine**[1,4]**, Emmanuel Barillot**[1,2,3]**, Andrei Zinovyev**[1,2,3‡]**, Laurence Calzone**[1,2,3‡]*

1 Institut Curie, Paris, France, 2 INSERM, U900, Paris, France, 3 Mines ParisTech, Fontainebleau, Paris, France, 4 CNRS UMR144, Paris, France

‡ These authors are joint senior authors on this work.
* laurence.calzone@curie.fr

Abstract

Understanding the etiology of metastasis is very important in clinical perspective, since it is estimated that metastasis accounts for 90% of cancer patient mortality. Metastasis results from a sequence of multiple steps including invasion and migration. The early stages of metastasis are tightly controlled in normal cells and can be drastically affected by malignant mutations; therefore, they might constitute the principal determinants of the overall metastatic rate even if the later stages take long to occur. To elucidate the role of individual mutations or their combinations affecting the metastatic development, a logical model has been constructed that recapitulates published experimental results of known gene perturbations on local invasion and migration processes, and predict the effect of not yet experimentally assessed mutations. The model has been validated using experimental data on transcriptome dynamics following TGF-β-dependent induction of Epithelial to Mesenchymal Transition in lung cancer cell lines. A method to associate gene expression profiles with different stable state solutions of the logical model has been developed for that purpose. In addition, we have systematically predicted alleviating (masking) and synergistic pairwise genetic interactions between the genes composing the model with respect to the probability of acquiring the metastatic phenotype. We focused on several unexpected synergistic genetic interactions leading to theoretically very high metastasis probability. Among them, the synergistic combination of Notch overexpression and p53 deletion shows one of the strongest effects, which is in agreement with a recent published experiment in a mouse model of gut cancer. The mathematical model can recapitulate experimental mutations in both cell line and mouse models. Furthermore, the model predicts new gene perturbations that affect the early steps of metastasis underlying potential intervention points for innovative therapeutic strategies in oncology.

Author Summary

We provide here a logical model that proposes gene/pathway candidates that could abrogate metastasis. The model explores the mechanisms and interplays between pathways that are involved in the process, identifies the main players in these mechanisms and gives some insight on how the pathways could be altered. The model reproduces phenotypes of published experimental results such as the double mutant Notch$^{+/+}$/p53$^{-/-}$. We have also developed two methods: (1) to predict genetic interactions and (2) to match transcriptomics data to the attractors of a logical model and validate the model on cell line experiments.

Introduction

Understanding the etiology of metastasis is very important in clinical perspective. Despite the progress with treatment of the primary tumours, the chances of survival for a patient decrease tremendously once metastases have developed [1]. It is estimated that metastasis accounts for 90% of cancer patient mortality [2]. It is now understood that the metastatic process follows a sequence of multiple steps, each being characterised by a small probability of success: 1) infiltration of tumour cells into the adjacent tissue, 2) migration of tumour cells towards vessels, 3) intravasation of tumour cells by breaching through the endothelial monolayer, 4) travelling in the circulatory or in the lymphoid system, 5) extravasation when circulating tumour cells re-enter a distant tissue, and 6) colonisation and proliferation in distant organs [3]. The early stages of invasion and migration are tightly controlled in normal cells and can be drastically affected by malignant mutations. It has been shown indeed that primary and secondary tumours have a common gene signature [4] that mediates the initial stages of metastasis while extravasation and colony formation by a (tumour) cell does not require malignant gene alterations [5], supporting the idea that the later stages of metastasis are affected by the anatomical architecture of the vascular system [6].

Here, we focus on the ability of cancer cells to infiltrate and migrate into the surrounding tissue. The first step towards the formation of secondary tumours is acquiring the ability to migrate. In order to gain motile capacity, epithelial cells need to change their morphology through Epithelial to Mesenchymal Transition (EMT), a process which occurs during development (EMT type 1), wound healing (EMT type 2) and under pathological conditions such as cancer (EMT type 3) [7,8]. EMT type 3 is characterised by both loss of E-cadherin (*cdh1*) and invasive properties at the invasive front of the tumour [9]. Gene expression of E-cadherin is inhibited by the transcription factors Snai1/2, Zeb1/2 and Twist1, while gene expression of N-cadherin (*cdh2*) is induced by the same transcription factors [8,10,11]. These transcription factors activate other genes that initiate EMT [11–13] and are induced by several signalling pathways including TGF-β, NF-κB, Wnt and Notch pathways [8,14,15]. On the contrary, the transcription factor p53 has been shown to inhibit EMT via degradation of Snai2 [16]; however, a p53 loss of function (LoF) alone is not sufficient to induce EMT [17]. After the switch of E-cadherin to N-cadherin expression, the cell-cell contacts are weakened [18,19] and cancer cells can pass the basal membrane to infiltrate the surrounding tissue [20]. The process of local invasion can be active since tumour cells can secrete Matrix Metalloproteinases (MMPs) that dissolve the lamina propria [21]. MMPs are also able to digest other components of the extracellular matrix (ECM) and thereby to release growth factors and cytokines that are attached to the ECM [21,22] which in turn activate the tumour cell's ability to propagate the dissolvement of the lamina propria. Finally, after dissolving the lamina propria and invading the (local)

stroma, cancer cells can migrate to distant sites by intravasation and extravasation of the vascular system [2]. To gain insight in the regulation of the metastatic process, several groups have developed mathematical models of various aspects of it [23–29] (S1 Text).

Our aim is to understand the role of gene alterations in the development of metastasis. In many (experimental or *in silico*) models, EMT is described as a very important step in acquiring metastasis and even considered to be synonymous to appearance of metastasis [30–32]. Due to EMT role in metastasis, much research has been performed to elucidate its regulation. The regulation of EMT is known to be complex and simple intuition is not sufficient to comprehend how genetic alterations (mutations and copy number variations) affect it. Logical modelling can give qualitative insight on how they could affect EMT and subsequently metastasis.

Previously, we have constructed a detailed map of molecular interactions involved in EMT regulation which is freely available at [33], and based on its structural analysis, we hypothesized a simple qualitative mechanism of EMT induction through upregulation of Notch and simultaneously deletion of *p53*. This prediction has been experimentally validated in a mouse model of colon carcinoma [31].

In the present study, we significantly extend the biological context and provide a mathematical framework for the description of the necessary conditions for having metastasis, going beyond the regulation of EMT only. We take into consideration the gained motility and ability to invade as determinants of the metastatic process. For this purpose we largely extended and re-designed the signalling network including more molecular players and phenotypes, and translated the network into a formal mathematical model, allowing prediction of the metastasis probability and the systematic analysis of mutant properties. Therefore, this work represents a significant progress with respect to the previous results, allowing reconsideration of the qualitative hypothesis suggested before using a formal mathematical modelling approach.

First, we introduce a logical model that recapitulates the molecular biology of the early steps in metastasis. The construction of the influence network and the choice of the logical rules are both based on knowledge derived from scientific articles. The final readouts of the model are the phenotype variables *CellCycleArrest*, *Apoptosis* and the aggregated phenotype *Metastasis* that combines the phenotypes *EMT*, *Invasion* and *Migration*.

We have chosen those final read-outs, as we believe that a metastatic phenotype depends on the occurrence of EMT, invasion and migration. In addition, apoptosis is of importance to the system as during healthy conditions, the cells undergo apoptosis when the cells detach from the basal membrane [34]. Suppressing apoptosis during migration is a required key feature. Our interest in cell cycle arrest is due to results of the mouse model [31] that show decreased proliferation. We try to model this feature in our logical model by looking at the regulation of cell cycle arrest. We did not focus on other phenotypes (or cancer hallmarks) such as proliferation explicitly, senescence, or angiogenesis. These are often considered in cancer studies but they were out of the scope of this work, which focused on depicting early invasion modes and not specifically on how tumour growth is regulated. The model inputs have been selected to represent external signals necessary for the metastasis initiation pathways. The Boolean model that we show here describes a possible regulation of the metastatic potential of a single tumour cell and not of multiple cells or a tissue.

We provide a simplified version of the model where some genes are grouped into modules (or pathways) allowing an analysis based on pathways rather than individual genes. Both versions of the models are validated by reproducing the phenotypic read-outs of published experimental mouse and cell line models.

We then analyse the two models and formulate several types of predictions: at the level of individual genes, e.g. exploring the individual role of each EMT inducer in metastasis; and at

the level of pathways, e.g. investigating the functional role of each pathway in triggering metastasis. The logical models can suggest a systematic mechanistic explanation for the majority of experimentally validated mutations on the local invasion and migration processes. Moreover, we were able to establish a link between the solutions of the mathematical model and the gene expression data from cell lines in which EMT was transiently induced. In addition, we have applied this method to the analysis of transcriptomes of tumour biopsies.

Lastly, we investigate how genetic interactions between different gene mutations can affect the probability of reaching a metastatic outcome. Our analysis predicts the effect of single mutations and the genetic interactions between two single mutations with respect to several cellular phenotypes. Our model proves an exceptionally efficient synergetic effect of increased activity of Notch in combination with a decreased activity of p53 on metastasis in accordance with our previous work [31].

Materials and Methods

The influence network

The construction of the influence network is based on scientific articles that describe the interactions between nodes of the model. We first selected the main genes or proteins that may contribute to activating EMT, regulating early invasion and triggering metastasis. We then searched for experimentally proven physical interactions that would link all these players, and simplified the detailed mechanisms into an influence network. For example, it has been shown experimentally that AKT protein phosphorylates and stabilises MDM2, which in turn inhibits p53 by forming a complex, leading to protein degradation of p53. We simplified the biochemical reactions by a negative influence from AKT to p53. The influence network is then translated into a mathematical model using Boolean formalism (see below for details). We verified the coherence of the network by comparing the outcome of the perturbed model to the observed phenotypes of mutants found in the literature. The final model is the result of several iterations that led to the accurate description of most of the published mutants related to the genes included in our model. Once the model was able to reproduce most of the published mutant experiments, we simulated mutants and conditions not yet assessed experimentally and predicted the outcome.

The Boolean formalism

From the *influence network* recapitulating known facts about the processes, we develop a mathematical model based on the Boolean formalism. To do so, we associate to a node of the influence network a corresponding *Boolean variable*. The variables can take two values: 0 for absent or inactive (OFF), and 1 for present or active (ON). The variables change their value according to a logical rule assigned to them. The *state of a variable* will thus depend on its *logical rule*, which is based on logical statements, i.e., on a function of the node regulators linked with logical connectors AND (also denoted as &), OR (|) and NOT (!). A *state of the model* corresponds to a vector of all variable states. All possible model states are connected into a *transition graph* where the nodes are model states and the edges correspond to possible transitions from one model state to another. The transition graph is based on asynchronous update, i.e., each variable in the model state is updated one at a time as opposed to all together in the synchronous update strategy. *Attractors* of the model refer to long-term asymptotic behaviours of the system. Two types of attractors are identified: *stable states*, when the system has reached a model state whose successor in the transition graph is itself; and *cyclic attractors*, when trajectories in the transition graph lead to a group of model states that are cycling. In this model, no cyclic attractors were found for the wild type case. However, we do not guarantee the non-existence

of cyclic attractors in some of the perturbed cases, as perturbations of the model may create new dynamics.

The logical rules

A logical rule is written for each variable of the model, corresponding to a node in the influence network, in order to define how its status evolves (ON or OFF). In this rule, the variables of the input nodes are linked by logical connectors according to what is known about their combined activities. There are several cases to consider: (1) The simplest logical rule that can be assigned is when a variable depends on the activity of a single input: for instance, the transcription factor Twist induces the transcription of the *cdh2* gene (see Table 1); (2) In the case of an input that has a negative effect on the activity of its target, the Boolean operator "NOT" or "!" is used: EMT is, for example, activated by CDH2 but inactivated by CDH1, thus for EMT to be activate, CDH1 should be OFF and CDH2 should be ON. The complete logical rule for the activation of EMT will be EMT = 1 (ON) if CDH2 &! CDH1 (see Table 1); (3) In some cases, a gene can be activated by two independent genes reflecting two different conditions and thus inputs are

Table 1. Logical rules describing the activity of a node.

Node	Rule
AKT1	CTNNB1 & (NICD | TGFbeta | GF | CDH2) & ! p53 & ! miR34 & ! CDH1
AKT2	TWIST1 & (TGFbeta | GF | CDH2) & !(miR203 | miR34 | p53)
CDH1	!TWIST1 & ! SNAI2 & ! ZEB1 & ! ZEB2 & ! SNAI1 & ! AKT2
CDH2	TWIST1
CTNNB1	!DKK1 & ! p53 & ! AKT1 & ! miR34 & ! miR200 & ! CDH1 & ! CDH2 & ! p63
DKK1	CTNNB1 | NICD
ERK	(SMAD | CDH2 | GF | NICD) & ! AKT1
GF	!CDH1 & (GF | CDH2)
miR200	(p63 | p53 | p73) & !(AKT2 | SNAI1 | SNAI2 | ZEB1 | ZEB2)
miR203	p53 & !(SNAI1 | ZEB1 | ZEB2)
miR34	!(SNAI1 | ZEB1 | ZEB2) & (p53 | p73) & AKT2 & ! p63 & ! AKT1
NICD	!p53 & ! p63 & ! p73 & ! miR200 & ! miR34 & ECM
p21	((SMAD & NICD) | p63 | p53 | p73 | AKT2) & !(AKT1 | ERK)
p53	(DNAdamage | CTNNB1 | NICD | miR34) & ! SNAI2 & ! p73 & ! AKT1 & ! AKT2
p63	DNAdamage & ! NICD & ! AKT1 & ! AKT2 & ! p53 & ! miR203
p73	DNAdamage & ! p53 & ! ZEB1 & ! AKT1 & ! AKT2
SMAD	TGFbeta & ! miR200 & ! miR203
SNAI1	(NICD | TWIST1) & ! miR203 & ! miR34 & ! p53 & ! CTNNB1
SNAI2	(TWIST1 | CTNNB1 | NICD) & ! miR200 & ! p53 & ! miR203
TGFbeta	(ECM | NICD) & ! CTNNB1
TWIST1	CTNNB1 | NICD | SNAI1
VIM	CTNNB1 | ZEB2
ZEB1	((TWIST1 & SNAI1) | CTNNB1 | SNAI2 | NICD) & ! miR200
ZEB2	(SNAI1 | (SNAI2 & TWIST1) | NICD) & ! miR200 & ! miR203
CellCycleArrest	(miR203 | miR200 | miR34 | ZEB2 | p21) & ! AKT1
Apoptosis	(p53 | p63 | p73 | miR200 | miR34) & ! ZEB2 & ! AKT1 & ! ERK
EMT	CDH2 & ! CDH1
Invasion	(SMAD & CDH2) | CTNNB1
Migration	VIM & AKT2 & ERK & ! miR200 & ! AKT1 & EMT & Invasion & ! p63
Metastasis	Migration

doi:10.1371/journal.pcbi.1004571.t001

linked by an OR, e.g., DKK can be activated either by CTNNB1 or by NICD, independently of each other; (4) In some other cases, two activators are linked by an AND connector, e.g., ZEB2 whose activity depends on several inputs including TWIST1 & SNAI2 which are needed simultaneously: it has been observed experimentally that both transcription factors Twist1 and Snai2 are required to induce gene expression of *zeb2*. All models are available in GINsim format in S1 File.

Computing phenotype probabilities using MaBoSS

MaBoSS is a C++ software for simulating continuous/discrete time Markov processes, defined on the state transition graph describing the dynamics of a Boolean network. The rates up (change from OFF to ON) and down (from ON to OFF) for each node are explicitly provided in the MaBoSS configuration file together with logical functions, which allows working with physical time explicitly. All rates are set to be 1 in this model since it is difficult to estimate them from available experimental facts. Probabilities to reach a phenotype are computed as the probability for the phenotype variable to have the value ON, by simulating random walks on the probabilistic state transition graph. The probabilities for the selected outputs are reported for each mutant based on predefined initial conditions (which can be all random). Since a state in the state transition graph can combine the activation of several phenotype variables, not all phenotype probabilities appear to be mutually exclusive. For example, *Apoptosis* phenotype variable activation is always accompanied by activation of *CellCycleArrest* phenotype variable (because p53 is a transcription factor of p21, responsible for cell cycle arrest, and the miRNAs, activated by the p53 and its family members, lead to a cell cycle arrest), and activation of the *Metastasis* phenotype variable is only possible when all three *EMT*, *Invasion* and *Migration* phenotype variables are activated.

With MaBoSS, we can predict an increase or decrease of a phenotype probability when the model variables are altered, which may correspond to the effect of particular mutants or drug treatments. If mutation A increases the *Apoptosis* probability when compared to the *Apoptosis* probability in wild type, we conclude that mutant A is advantageous for apoptosis. All models are available in MaBoSS format in S1 File.

Module activity

The pathway activity (synonymously, module activity) score in a tumour sample is defined as the contribution of this sample into the first principal component computed for all samples on the set of the module target genes, as it was done in [35]. This way, we test target gene sets selected from MSigDB [36] and KEGG [37] databases together with few tens of gene sets assembled by us from external sources. The gene lists for each module is provided in S5 Table. Differential activity score of each module was estimated by t-test between metastatic and non-metastatic groups and significantly active/inactive modules were selected according to p-value <0.05 condition.

Transcriptomics data for tumour samples

We conducted our study on the publicly available data of human colon cancer from TCGA described in [38]. By excluding rectal cancers from the original dataset, the remaining 105 tumour samples were included in our analysis, classified into two groups ('*metastatic*' M1 = 17 tumours and '*non-metastatic*' M0 = 88 tumours) according to clinical information about metastasis appearance during cancer progression.

Transcriptomics data for cell lines

We used gene expression data generated from A549 lung adenocarcinoma cell line that was treated with TGF-β1 ligand at eight different time points [39]. In short, gene expression was measured for three replicates at each time point using Affymetrix Human Genome U133 Plus 2.0 Array. For more information about treatment and growth protocols see [40].

Matching transcriptomics data to logical steady states on EMT-induced cancer cell lines

We followed the following six steps to link transcriptome data to the stable states of the model (described in detail in S2 Text): (1) We first matched the genes of the model with their HUGO names. For phenotypes such as *Apoptosis*, *Migration* or *Invasion*, the genes coding for CASP9, CDC42, and MMP2 were used as biomarkers, respectively. These readouts were selected as the most representative of the process; they were chosen based on the changes of the expression of a list of candidate genes we explored throughout the experiments. (2) We averaged the genes over the 3 replicates for time point T0 (initiation of experiment with no TGF-β), for T8 (identified as the beginning of EMT), for T24 (EMT in process) and for T72 (last point). (3) Using several methods (binarization algorithms available in [41]), we identified a threshold of expression and binarized the data accordingly. Among our list of genes, only 11 of them have significant expression dynamics along the experiment: *cdh1*, *cdh2*, *ctnnb1*, *egfr*, *mapk1*, *mmp2*, *smad3*, *snai2*, *tgfb1*, *vim* and *zeb1*. The other genes were either always ON or always OFF throughout the 72 hours of experiments because the expression is either above or below the threshold we set. (4) We associated a label (phenotype) to the 9 stable states of the logical model based on the activity status of the phenotype variable. (5) The similarity matrix was computed according to the following rule: for each stable state and for each time point, if a gene is ON (= 1) or OFF (= 0) in both the vector of discretized expression data and the vector of the stable state, we set the entry in the similarity matrix to 1, otherwise, it is set to 0. (6) For each time point and each stable state, we then summed up the corresponding similarity matrix row, and set an expression-based phenotypic (EBP) score for each stable state. The highest EBP score for each time point corresponds to the phenotype that is the closest to the studied sample and is representative of the status of the cells.

Non-linear principal component analysis by elastic maps method

The non-linear principal manifold was constructed for the distribution of all single and double mutants of the model in the space of computed model phenotype probabilities, using elastic maps method and ViDaExpert software [42–44]. We preferred using a non-linear version of principal component analysis (PCA) for data visualisation in this case, because it is known to better preserve the local neighbourhood distance relations and allows more informative visual estimation of clusters compared to the linear PCA of the same dimension [42]. For data analysis, only those "mixed" phenotypes were selected whose probability expectation over the whole set of single and double mutants was more than 1%. It resulted in a set of 1059 single and double mutants embedded into 6-dimensional space of phenotype probabilities for which the principal manifold was computed.

Synthetic interactions with respect to metastatic phenotype

The results of double mutants were used to quantify the level of epistasis between two model gene defects (resulting either from gain-of-function mutation of a gene or from its knock-out or loss-of-function mutation) with respect to metastatic phenotype. The level of epistasis was

quantified using the simplest multiplicative null model applied for the event of *not having* metastasis: $\varepsilon = (1-p_{12})-(1-p_1)(1-p_2)$, where p_1 and p_2 are the probabilities of having metastasis in single mutants, and p_{12} was the probability of having metastasis in the double mutant. Therefore, negative values of the epistasis score E correspond to synergistic interactions when two gene defects amplify each other's effect stronger than expected in the multiplicative model. On the contrary, positive values correspond to alleviating effect, when the effect of one gene defect could be masked (sometimes, even reduced to zero) by the second mutation. For genetic network visualisation, we kept the most significant interactions with $\varepsilon < -0.2$ or $\varepsilon > 0.3$ values. These thresholds were chosen because at these levels we observed gaps in the distribution of ε values. The complete list of interactions together with p_1, p_2, p_{12} and ε values can be found as a Cytoscape 3 session (S2 File).

Results

Construction of an influence network regulating EMT, invasion and cell migration

Mesenchymal cells are characterised by their increased motility, loss of *cdh1* (coding for E-cadherin) expression, increased expression of *cdh2* (coding for N-cadherin), and presence of *vimentin* (Vim) [7,10,45]. The EMT program can be initiated by the transcription factors *snai1*, *snai2*, *zeb1*, *zeb2* and *twist1*. They are considered to be the core regulators of EMT as each has been shown to down-regulate *cdh1* [46–50]. In turn, the genes coding for these core EMT-regulators are subjected to regulation by other signalling pathways. The TGF-β pathway has been reported to be able to induce EMT [7,51], but other pathways are also involved in EMT including Wnt, Notch and PI3K-AKT pathways [52–56].

Furthermore, microRNAs regulate the Snai and Zeb family members. For example, miR200 targets *snai2*, *zeb1* and *zeb2* mRNA [57–59] whereas miR203 targets *snai1* and *zeb2* mRNA [59], and miR34 targets *snai1* mRNA [60]. The transcription of these microRNAs is under the control of p53 [61–64]. The miR200 expression can also be induced by p63 and p73 proteins, while miR34 is only induced by p73 but is down-regulated by p63 [65–67]. The microRNAs can be down-regulated by the EMT-inducers Snai1/2, and Zeb1/2 [59,60,68]. Note that the proteins p63 and p73 have been identified as members of the p53 protein family since their amino acid sequences share high similarity with that of p53 [69]. They are able to bind to the promoters of the majority of the p53-target genes and therefore have overlapping functions in cell cycle arrest and apoptosis [70,71]. The p53-family members are involved in cross-talks with Notch and AKT pathways: p63 protein is inhibited by the Notch pathway, p53 by AKT1 and AKT2 [69,72–76] while p73 is down-regulated by p53 (itself negatively regulated by p73), AKT1, AKT2, and Zeb1 [69,72,77].

The PI3K-AKT pathway has been considered to be important in evading apoptosis and cell cycle arrest by modulating the TRAIL pathway, down-regulating pro-apoptotic genes and phosphorylating p21 [78–80]. More recently, AKT has been assigned additional but important roles in the development of metastasis. AKT1 suppresses apoptosis upon cell detachment (anoikis) of the ECM [34]. The different isoforms of AKT seem to have opposing roles in the regulation of microRNAs: AKT1 inhibits miR34 and activates miR200 while AKT2 inhibits miR200 and activates miR34 [81]. Another opposing role for both AKT isoforms has been found in migration. AKT1 inhibits migration by phosphorylating the protein Palladin; phosphorylated Palladin forms actin bundles that inhibit migration. AKT2 increases the protein Palladin stability and upregulates β1-integrins stimulating migration [82,83] or by inhibiting TSC2 that, in turn, activates RHO [84]. Furthermore, AKT1 inhibits cell cycle arrest while AKT2 activates it [85,86] (all these effects are shown implicitly in Fig 1A).
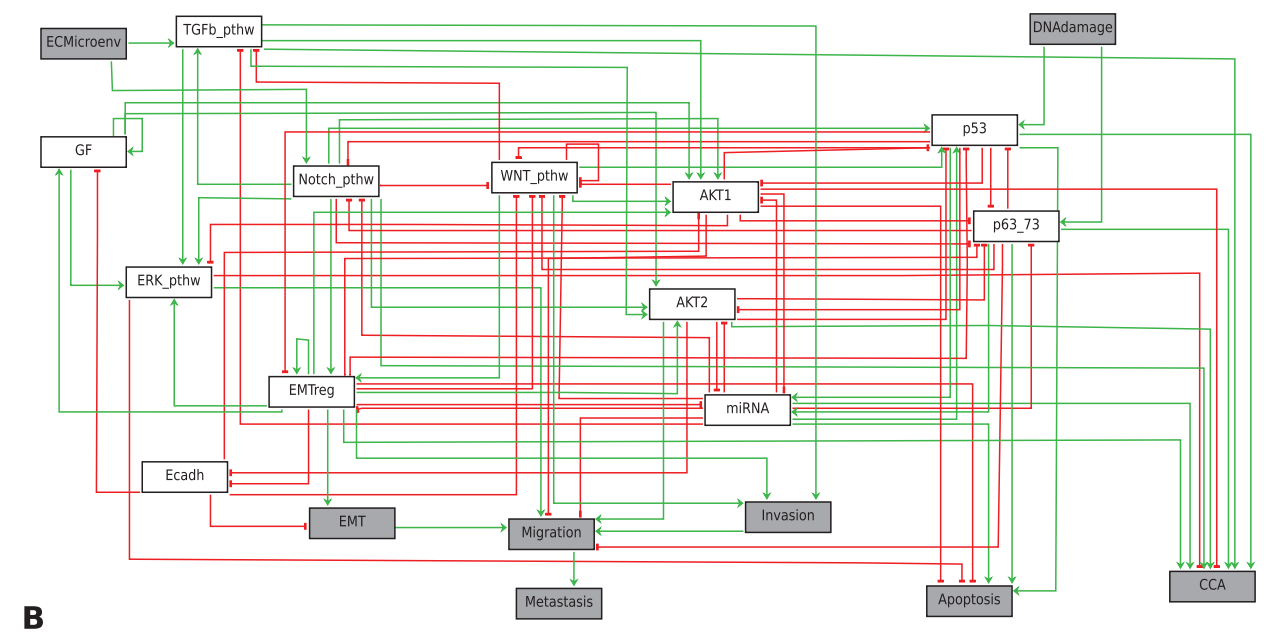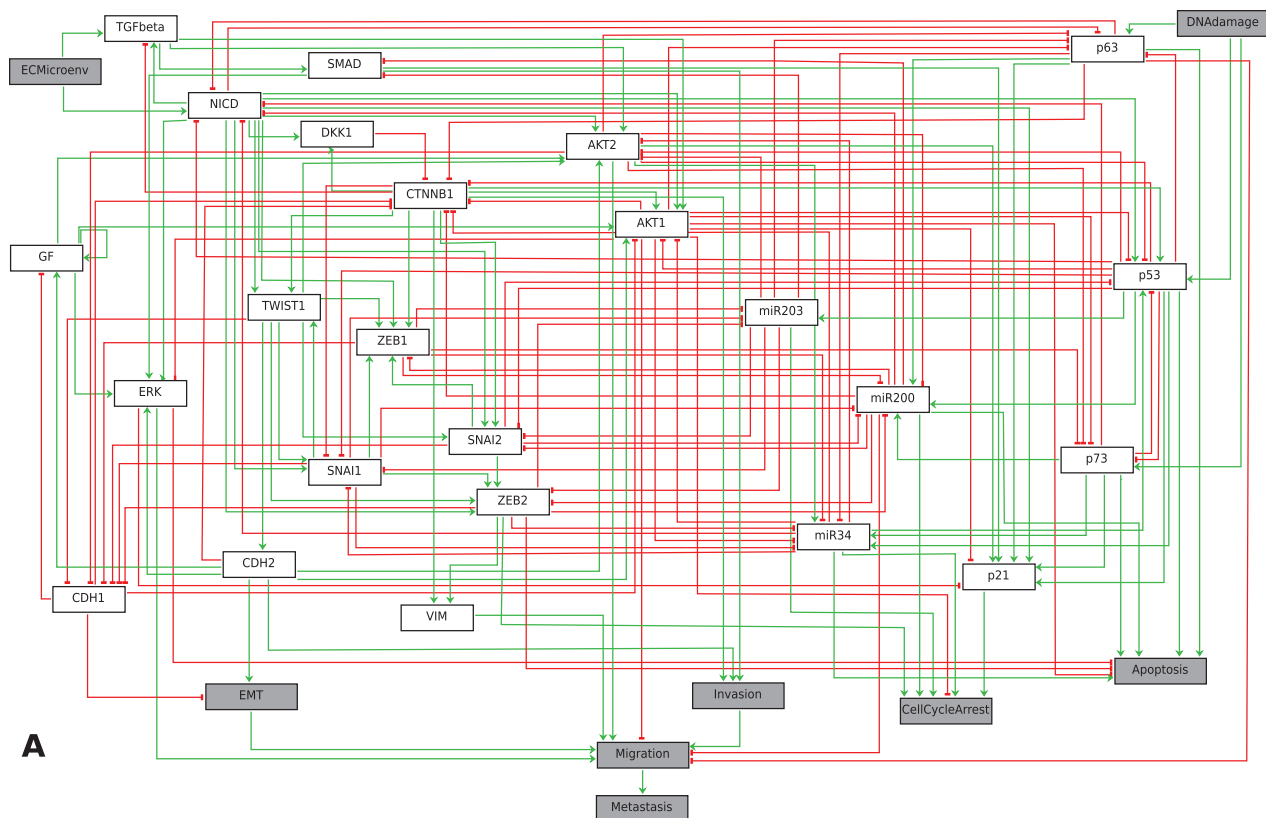
Fig 1. Regulatory networks of mechanisms leading to EMT, invasion, migration and metastasis. A. Detailed network of the pathways involved in metastasis. B. Modular network derived from network in A.

doi:10.1371/journal.pcbi.1004571.g001

Extracellular stimuli are also included in the logical model. Growth factors (GF) are soluble ligands that can be excreted locally or from longer distances and are able to activate the PI3K-AKT, and MAPK pathways [87,88]. Another extracellular stimulus might be the extracellular microenvironment (ECMicroenv) with components that are not soluble including the extracellular matrix. The ligands for the TGF-β pathway can be imbedded in the extracellular matrix [89–91] and the ligands for the Notch pathway are transmembrane proteins from adjacent neighbouring cells [92,93].

These mechanisms are depicted in an influence network (Fig 1A). The network is composed of nodes and edges, where some nodes represent biochemical species (proteins, miRNAs, processes, etc.) and others represent phenotypes, and edges represent activating (green) or inhibitory (red) influences of one node onto other node. Each edge is annotated and supported by experimental papers (see S1 Table). Throughout the article, we will use the general term "phenotypes" to refer to "phenotype variables", which correspond to the four outputs: *CellCycleArrest*, *Apoptosis*, *Metastasis* (depending on *EMT*, *Migration* and *Invasion*), and Homeostatic State (HS) as presented below.

Mathematical modelling of the influence network

Construction of a logical model and its stable states. The network of Fig 1A is translated into a logical model using GINsim software [94]: a logical rule is assigned to each node of the network (Table 1, and Materials and Methods). Once the logical rules are set for each node of the network, the Boolean model can simulate solutions or outcomes that correspond to attractors in the state transition graph (see Materials and Methods for details). The model, for the wild type condition (i.e. no mutations or gene alterations), counts nine stable states for all combinations of inputs (Table 2). To each stable state, a phenotype is assigned based on the genes that are activated (variable is ON, thus equal to 1). The phenotypes identified are: *CellCycleArrest* together with *Apoptosis*; *CellCycleArrest* together with *EMT*; *Metastasis* (depending on three other processes: *EMT*, *Migration* and *Invasion*); and a stable state with only Cdh1 ON. This state corresponds to a state where metastasis is inhibited by Cdh1 activity. We refer to it as the homeostatic state (HS). It is a particular state of an epithelial cell that is not explicitly represented as a phenotype variable in this mathematical model. Four out of the nine stable states lead to *Apoptosis*, in the presence of DNA damage and absence of growth factors (GF). Two stable states show an *EMT* phenotype alone (without inducing *Metastasis*). In these stable states, *Invasion* and *Migration* are not activated because TGF-β pathway is not initially ON. The last two stable states lead to *Metastasis* in the presence of growth factors. GF activates the ERK pathway that switches off the p53-family targets and permits the triggering of events leading to metastases. Indeed, several studies have shown the importance of ERK in migration [95–97].

Testing robustness of the model with respect to small changes in the logical rules. We systematically checked the effect of changing the logical operators of the model from "OR" to "AND", and vice versa, onto the resulting model phenotype probabilities. More specifically, we generated model variants with one change of a logical operator in one logical rule, two changes in the same logical rule, or one single change in two different logical rules, leaving the rest of logical operators the same as in the wild type model. Therefore, we considered all model variants different from the wild type model by at most two different logical operators. The analysis resulted in 8001 model variants.

We first show that the distributions of phenotype probabilities after these changes are concentrated around the wild type probability values (S6 Fig).

Metastasis appeared to be the least robust model phenotype, which confirms the fact that there are some necessary conditions that need to be met to lead to metastasis (illustrated by

Table 2. The nine stable states of the mathematical model. The label of the columns corresponds to the phenotypic outputs.

	HS	Apop1	Apop2	Apop3	Apop4	EMT1	EMT2	M1	M2
Metastasis	0	0	0	0	0	0	0	1	1
Migration	0	0	0	0	0	0	0	1	1
Invasion	0	0	0	0	0	0	0	1	1
EMT	0	0	0	0	0	1	1	1	1
Apoptosis	0	1	1	1	1	0	0	0	0
CellCycleArrest	0	1	1	1	1	1	1	1	1
ECMicroenv	0	0	0	1	1	0	0	1	1
DNAdamage	0	1	1	1	1	1	0	1	0
GF	0	0	0	0	0	1	1	1	1
TGFbeta	0	0	0	1	1	0	0	1	1
p21	0	1	1	1	1	0	0	0	0
CDH1	1	1	1	1	1	0	0	0	0
CDH2	0	0	0	0	0	1	1	1	1
VIM	0	0	0	0	0	1	1	1	1
TWIST1	0	0	0	0	0	1	1	1	1
SNAI1	0	0	0	0	0	1	1	1	1
SNAI2	0	0	0	0	0	1	1	1	1
ZEB1	0	0	0	0	0	1	1	1	1
ZEB2	0	0	0	0	0	1	1	1	1
AKT1	0	0	0	0	0	0	0	0	0
DKK1	0	0	0	0	0	0	0	1	1
CTNNB1	0	0	0	0	0	0	0	0	0
NICD	0	0	0	0	0	0	0	1	1
p63	0	0	1	0	1	0	0	0	0
p53	0	1	0	1	0	0	0	0	0
p73	0	0	1	0	1	0	0	0	0
miR200	0	1	1	1	1	0	0	0	0
miR203	0	1	0	1	0	0	0	0	0
miR34	0	0	0	0	0	0	0	0	0
AKT2	0	0	0	0	0	1	1	1	1
ERK	0	0	0	0	0	1	1	1	1
SMAD	0	0	0	0	0	0	0	1	1

doi:10.1371/journal.pcbi.1004571.t002

AND operators in the logical rules). If approximately 49% of changes in the logical rules have minor or no effect onto the *Metastasis* phenotype probability, some modifications in some rules changed the *Metastasis* phenotype to zero (implicating p63, p73, AKT1 variables of the model and, to a lesser extent, CTNNB1, miR34, p53). Most of the rules that concern these variables are indeed more stringent. A change from an AND gate to an OR gate for the case of p63 or AKT1 has an important impact on the metastasis process. For instance, if p63 is more present, because it is inactivated with fewer constraints, it can block more easily migration and thus, metastasis. These logical rules should be considered more carefully than the others because a mistake in defining these rules can have more drastic effects on the model properties than any other modifications.

We also performed a reproducibility analysis of individual logical stable states in the models differing from the wild type model by one or two changes in the same logical rule or one change in two logical rules as presented above. The wild type model is characterized by nine

stable states, including the homeostatic state (HS) (see Table 2). 8001 model variants mentioned above are characterized by 68726 stable states counted in total. Hence, in average, each model variant is characterized by 8 or 9 stable states, which might be different from the wild type model. In total, we have counted 1176 distinct stable states in all the 8001 model variants, observed with different frequencies (S6 Table). The nine stable states of the wild type model are robustly reproducible, being the most frequently observed stable states, and accounting for 59% of all observed stable states in different model variants. Another 13% of observed stable states differ from one of the wild type stable states by only one change in the Boolean variable values (DIST_TO_WT = 1). Some modifications of logical rules for CTNNB1 or NICD lead to very rarely observed atypical but very different from the wild type stable states (DIST_TO_WT = 12). Based on all these analyses, we conclude that the nine wild type model stable states are robust and "typical" with respect to moderate random modifications of the logical rules and fragile to few targeted modifications.

Model reduction into a modular network. To make our modelling more insightful, we reduced the complexity by lumping variables into modules corresponding to signalling pathways: the TGF-β pathway (TGFb_pthw consisting of TGFbeta, SMAD), Notch pathway (Notch_pthw, includes activated Notch intracellular domain (NICD), the WNT pathway (WNT_pthw consisting of DKK1, CTNNB1), the p53 pathway (p53, consisting of p53), the p63-p73 proteins (p63_73 consisting of p63 and p73), the miRNA (miR34, miR200, miR203), the EMT regulators (EMT_reg including Twist1, Zeb1, Zeb2, Snai1, Snai2, Cdh2, Vim), E-cadherin (Ecadh with Cdh1), growth factors (GF), the ERK pathway (ERK_pthw: ERK), p21 is included in the *CellCycleArrest* phenotype, AKT1 module and AKT2 module. In the reduced model (Fig 1B), the inputs (ECMicroenv and DNAdamage) and (final and intermediate) outputs (*Migration*, *Invasion*, *Metastasis*, and *Apoptosis*) are conserved. The reduced model produces the same stable states (for the wild type conditions) as those of the initial model (Fig 1A, see S4 Text).

Validation of the Boolean model. We simulated the genetic perturbations that correspond to published experimental settings and verified that the stable states of the mathematical model correspond to the experimental observations. An overexpression or gain of function (GoF) of a gene is simulated by forcing the value of the node to ON and a deletion or loss of function (LoF) by forcing the value of the node to OFF. We first simulated not only previously described mutants but also mutants that have not yet been experimentally validated (see S4 Table). The mathematical model is able to reproduce the experimental results of almost all described mutants. In few cases, there is a discrepancy between the mathematical and the biological model due to three reasons described below: 1) Metastasis in our logical model is defined as colonisation of tumour cells into distant organs through migration in the systemic and/or lymphatic vessels. A limitation of the cell line model is that a metastatic output cannot be measured. 2) Dosage-dependent effects cannot be modelled using the logical formalism. For example, our model predicts metastasis in a *kras* GoF while the mouse model does not develop distant metastatic tumours. A possibility for the difference is that in the mouse model the wild type *kras* allele is still present (a heterozygous mutation) while in our model KRAS mutant is homozygous. It has been reported that the remaining wild type *kras* gene has still tumour suppressive properties: it can reduce tumourigenesis in lung [98,99] and in colon cancer cell line by inhibiting proliferation [100]. Other studies in cancer cell lines that are heterozygous for *kras* mutation showed that the wild type *kras* gene in those cell lines decreased the migration and colonisation capacity [101,102] suggesting a dose-dependent effect [103]. This might indicate that mouse mutants homozygous for *kras* mutation may develop distant metastasis as predicted by our mathematical model. 3) Simulating mutations of genes that are not explicitly represented as a node in the model has its limitations because the network does not describe

exactly the function of such node. For example, even though PTEN is not a variable of our model, we simulated a *pten* mutation to understand the controversial results of such deletion on metastasis in experimental models. The *pten* LoF mutations have been associated with many different types of cancers [104–106] and recently it has been demonstrated that *pten* mutations cause genomic instability [107,108]. In our model, in order to simulate a PTEN LoF, its two targets, AKT1 and AKT2, are forced to be ON: PTEN inhibits activation of AKT isoforms [109–111]. The model predicts that a PTEN LoF alone or in combination with gene mutations will reach the stable states without having metastasis while metastasis is observed in the mouse model. In our model, due to activation of AKT1 by the PTEN LoF, metastasis is prevented, because AKT1 inhibits migration as mentioned before. A recent study indicates that in PTEN-deficient tumours, AKT2 is the active isoform [112] but not AKT1. The model confirms this study: when we simulate the single AKT2 activation as a result of PTEN LoF, the model predicts a stable state in which metastasis can be reached (All references and model results are available in S4 Table).

Role of different pathways/modules in triggering metastasis

To assess the importance of each pathway on metastasis, apoptosis and cell cycle arrest, we simulated a gain of function or a loss of function, in the reduced model, for each module and for all combinations of inputs. These simulations mean that when an important entity in a pathway is altered, it affects the whole pathway activity. The model shows that mutations leading to either GoF or LoF of each pathway have opposing results in the occurrence of migration and for the occurrence of metastasis (S2 Table). The Notch_pthw is an exception in this: both a GoF and LoF of the Notch pathway can lead to a stable state solution with metastasis ON. This might indicate that Notch (pathway) activity must be in a certain range in order to have a non-pathological effect or that Notch is important for the functioning of some dynamic feedback controls preventing metastasis (so fixing it at a particular value would destroy these feedbacks). In addition, GoF of the Notch_pthw, TGFb_pthw, ERK_pthw, EMT_reg or AKT2 shows their inhibitory role in the apoptotic process as it has been demonstrated before [113–117]. For the p53, TGF-β, EMT_reg and miRNA pathways, mutations leading to activation or inhibition have opposing results in regulating invasion when either the pathway is activated or inhibited. This effect on invasion is a direct result of having an activating or inhibiting role on EMT except for the TGF-β pathway.

The role of TGF-β pathway has been investigated. The activation of TGF-β pathway might be dependent on the micro-environment as its ligands can be found in the extracellular matrix [89–91]. The triple mutant: Notch_pthw GoF, p53 LoF and TGFb_pthw LoF leads to one stable state in which the EMT_reg is ON but no metastasis, migration, invasion or apoptosis are reachable (S2 Table) indicating that activation of TGF-β pathway (e.g., by the peripheral tumour cells more exposed to the micro-environment) is required to have metastasis in the double mutant by activating invasion [118,119].

Comparing the Boolean model with dynamical transcriptomic data on EMT induction and tumoral transcriptomes. In this section, the aim is to investigate if the model can predict temporal trends in the dynamics of high-throughput data in cancer cell lines or to retrospectively predict a possible appearance of metastasis using the model. Is it possible to correlate experimental or clinical data to the stable states of the model?

We first analysed the publicly available colon gene expression dataset generated by The Cancer Genome Atlas (TCGA) project [38]. Student t-test between metastatic and non-metastatic tumours was performed for genes included in the influence network to identify significant changes in their expression between the two groups (S1 Fig). Few significant

differences were observed in the expression of the influence network genes in these two groups. Moreover, there was no significant differential expression of the EMT regulators observed between the two groups: expression of the EMT regulators seems to be OFF in these tumours. Since single gene-based analysis of colon cancer did not show significant differential changes in the expression of the influence network genes, we investigated the expression of the downstream targets for the transcription factors in the modular network (Notch_pthw, p53, p63_p73, EMT regulators, etc.) and recapitulated their expression into a pathway activity score (see Methods). The assumption was that the differential activity of a given transcription factor can be better reflected by a score based on the expression of its target genes rather than from its own individual expression. For the nodes that are not transcription factors (AKT1, AKT2, etc.) we considered all genes involved in the same network module. We observed that the targets of Notch pathway, Wnt pathway, p63_p73, and AKT1 and AKT2 downstream genes showed significantly higher activity score in metastatic compared to non-metastatic samples whereas p53 and microRNAs targets were less active in metastatic samples. However, the EMT regulator module showed almost no difference in module activity even if all regulators were combined in one module (See S2 and S3 Figs). Indeed, in the recent colorectal tumour-specific EMT signature established by Tan *et al.* [120] none of the genes of our EMT module were included. This means that at least in the colorectal cancer, the transcriptional dynamics of the EMT genes has relatively small amplitude, when measured on the bulk of the tumour.

Based on our analysis, we hypothesize that only a small portion of the tumour cells in a tumour sample are undergoing EMT and as a result, the EMT signal is strongly diluted when looking at the whole cell population in a sample taken from the tumour bulk. This low signal to noise ratio is not favourable to study the dynamics of the EMT process, and subsequently, the metastatic process.

We thus analysed publicly available transcriptomics data from cancer cell lines in which EMT has been induced. In a study conducted by Sartor and colleagues [39], lung carcinoma cell lines were administered with increasing amount of TGF-β and genome-wide transcriptome was measured at eight different time points, following the induction of EMT. The induction of EMT was accompanied by increasing expression for some of the EMT regulators (S4 Fig).

The expression of these regulators follows a sigmoid curve in response to TGF-β induction. For a given time-point, we checked if the expression level of the components of our model could be associated to a particular steady state of the model. We expect our model to reflect the behaviour of EMT expression level at early or late time points.

We then determined the consistency of the EMT induction experiment with the logical model following the steps presented in Materials and Methods section (and in S2 Text for details of each step). The resulting EBP (expression-based phenotypic) score of the method represents how similar an experimental condition is to a stable state. Thus, the higher the EBP score for a stable state is, the more similar the data are to that stable state, and as an extension, to the phenotype variable associated to that stable state. The computed EBP scores at each time point illustrate the evolution of the data in terms of the stable states. At T0, the highest EBP score is associated with apoptosis. At T8, both metastasis and apoptosis stable states have the highest EBP score illustrating the balance of phenotypes observed in the gradual entry into EMT. At T24 and at T72, the metastatic phenotype has the highest EBP score suggesting that EMT has occurred. Based on the above-mentioned results, the logical model is in accordance with the time course experiments in EMT-induced cell lines.

With this similarity EBP score, we have developed a method to characterise tumours in terms of a particular biological process (how the metastatic process follows EMT, migration and invasion here) with respect to the solutions of a logical model.

Role of individual EMT regulators in triggering metastasis

To identify for each EMT regulator (Snai1, Snai2, Zeb1, Zeb2, Twist1) their specific role in the different cell fates considered in our model, we simulated LoF and GoF mutants and observed that all GoF, except for that of Snai2, led to the loss of apoptosis (S3 Table). *Metastasis* can be reached for all GoF mutants but other phenotypes can still be reached depending on the combinations of inputs. The single deletions of each EMT regulator show that Zeb2 and Twist1 are required for metastasis. Zeb2 controls migration mainly through VIM but has no direct impact on invasion. Twist1 LoF, on the contrary, modulates negatively the possibility to reach not only the metastatic phenotype but also EMT, migration and invasion. Twist1 controls EMT through Cdh2 that controls migration and EMT. Other factors, such as CTNNB1 (β-catenin) or TGF-β, play a role in triggering the metastatic process by modulating invasion or migration, but our model suggests that the main EMT regulators are Zeb2, Twist1 or Snai2, either as loss of function for Zeb2 and Twist1, or gain of function for Snai2. Note that by definition, Cdh2 is absolutely required for metastasis to occur because of its direct role in controlling EMT and migration. In our model, Cdh1 inhibits EMT (directly) and migration (through CTNNB1 and VIM) but not invasion. Since all three phenotypes are required for metastasis, the process is thus impaired when Cdh1 is over-expressed [121,122].

Modelling synthetic interactions between genes composing the model

The probability of achieving the metastatic phenotype for all possible single and double mutants was systematically computed using MaBoSS [123]. Each single and double mutant is characterised by the distribution of phenotype probabilities. A non-linear PCA analysis was performed as described in Methods, which allowed to group together single and double mutants having similar effect on the model phenotypes (Fig 2A). In this plot, one can

Fig 2. A. Genetic interactions between two mutants leading to the masking or the antagonism of a phenotype (metastasis). Application of non-linear dimension reduction for visualising the distribution of phenotype probabilities, computed with MaBoSS for all single and double mutants of the model. The grading in the background shows the density of points (mutants) projections. Six clusters are distinguished based on this grading. Wild-type model, all single over-expression and knockout mutants and the NICD GoF / p53 LoF mutant are labelled. Note that each gene pair in this plot is represented by four different double mutants (small red points) corresponding to LoF/LoF, LoF/GoF, GoF/LoF, GoF/GoF combinations. B. Genetic interaction network showing the most significant synergistic (shown in green) and alleviating (masking, showing in red) interactions between GoF and LoF mutants with respect to the probability of having metastasis. The size of the node reflects the metastasis probability for individual mutation. The thickness of the edge reflects the absolute value of epistasis measure (see Methods).

distinguish six major clusters (a to f) which can be tentatively annotated as "almost wild-type" (no significant changes in the phenotype probabilities compared to the wild-type model), "risk of metastasis" (elevated probability of having metastasis though not equal to 1), "apoptotic" (for these mutants *Apopotosis* and *CellCycleArrest* phenotypes are activated), "EMT without migration" (for these mutants, presented as two clusters, the formation of metastases cannot be accomplished because the cells did not acquire ability to migrate), "cell cycle arrest only" (these mutants are found arrested without starting EMT or invasion or apoptotic programs). The direction of increased metastasis probability is shown by dashed line in Fig 2A, which ends at NICD GoF/p53LoF double mutant for which the probability of having metastasis equals to 1, according to the model (whereas single p53 LoF mutation belongs to "almost wild type" and single NICD GoF mutation belongs to "risk of metastasis" clusters respectively).

Synthetic interactions with respect to metastatic phenotype. The most significant genetic interactions with respect to probability of having metastasis (see Methods) are shown in Fig 2B. The following observations can be made: (1) Hubs in this genetic interaction network are the genes for which a single mutation (GoF) leads to a significant increase in having the metastatic phenotype. These genes are *akt2*, *twist1*, *snai1*, and *snai2*; (2) There are a number of genes whose LoF or GoF lead to a significantly masking effect on the phenotype caused by the hub-gene mutations (red edges in Fig 2B). For example, overexpression of *p53* gene or knockout of *erk* gene drastically decreases the probability of metastatic phenotype in SNAI1 LoF mutant; (3) There are relatively few synergistic effects observed between single mutants (green edges in Fig 2B). Some of them have been experimentally performed while other synergistic interactions are rather unexpected such as GoF for both AKT2 and NICD, and can be a subject of further experimental work.

There are four synergistic interactions, which result in augmenting the probability of having metastasis to 100%. First, two of them are combinations of NICD GoF and p53 LoF (NICD$^+$/p53$^-$), or simultaneous NICD GoF and p73 GoF (NICD$^+$/p73$^+$). These two interactions can be considered as being dependent, since overexpression of p73 leads to downregulation of p53 function [124,125]. The other two interactions (SNAI2 GoF and NICD GoF, AKT2 GoF and NICD GoF) are potential amplifier mechanisms for appearance of metastasis in NICD GoF mutant alone.

In addition, we classified all gene pairs into five large clusters according to four different combinations of *in silico* mutation types (LoF/LoF, LoF/GoF, GoF/LoF, GoF/GoF). Inside each cluster, the gene pairs can be ranked according to the strength of the activating effect of one of the mutation combinations on the *Metastasis* phenotype (S5 Fig). Moreover, all gene pairs can be ranked according to the amplitude, i.e. the difference between the maximal and minimal metastatic phenotype probabilities among four values (LoF/LoF, LoF/GoF, GoF/LoF, GoF/GoF). The most distinguished gene pair in this analysis is p53/NICD, which is a unique and extreme case of the gene pair cluster when any combination of mutation types besides LoF/GoF makes the metastatic phenotype non-reachable (zero or close to zero probability) while the synthetic-dosage interaction LoF/GoF makes the metastatic phenotype unavoidable (probability one) (cluster 3 in S5 Fig).

Synthetic dosage interaction between Notch and p53 genes. Using MaBoSS, we have been able to quantify the changes of probabilities for reaching each phenotype relative to the wild type model. We are thus interested in results such as: "more or less apoptosis than in wild type". We simulated three mutants with MaBoSS: p53 LoF (Fig 3B), NICD GoF (Fig 3C) and the double mutant NICD$^+$/p53$^-$ (Fig 3D). These simulations are of particular interest since they show an example of genetic interaction predicted to have the probability of metastasis phenotype equals to 1, as presented above.
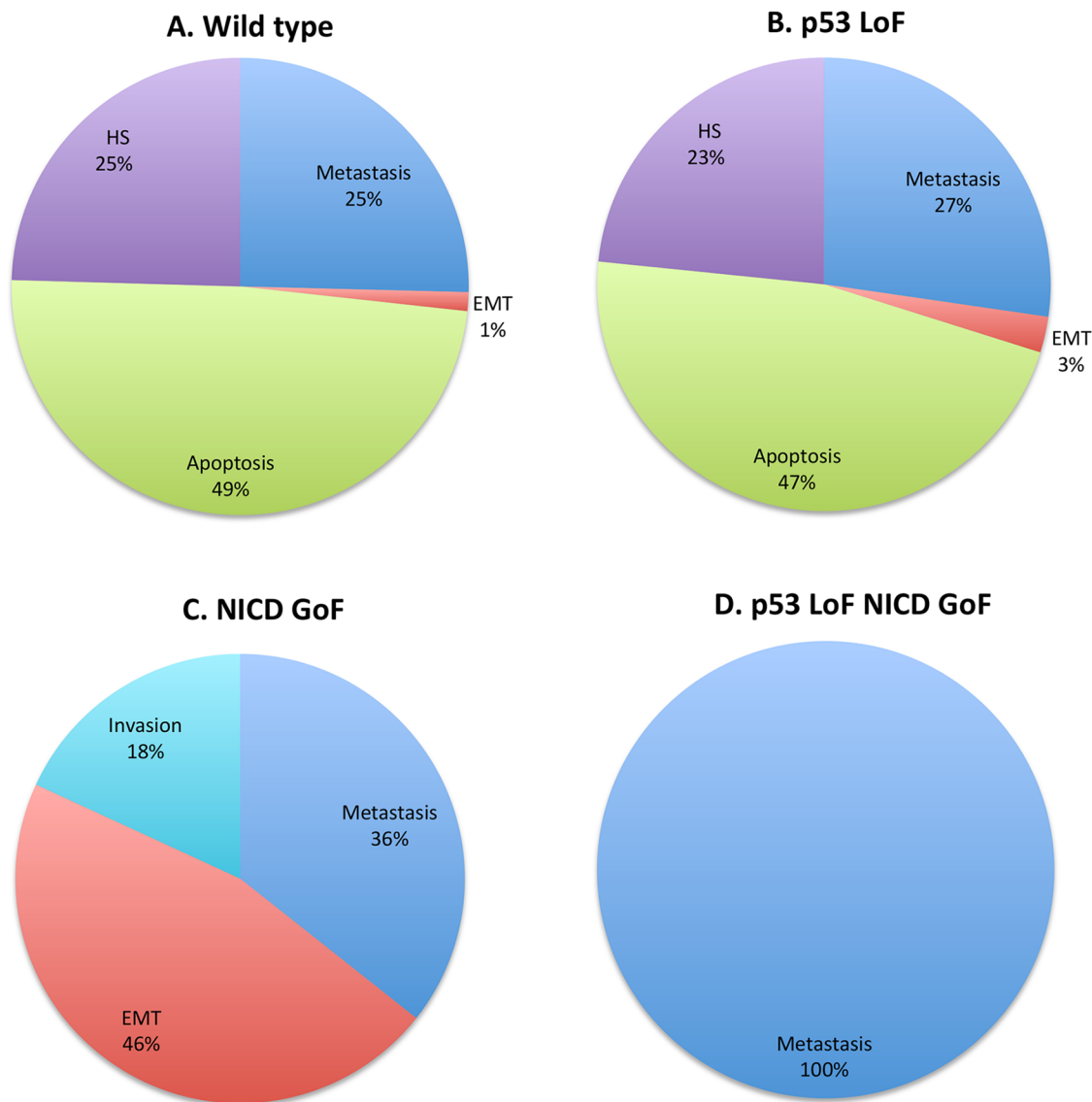
Fig 3. MaBoSS simulation of wild type, of individual mutations of p53 and NICD and of the double mutant. The probabilities associated with each phenotype represent the number of stochastic simulations leading to each phenotype from pre-defined initial conditions. A. Wild type, see text. B. p53 LoF, same phenotypes found in (A) are reachable but with different probabilities than wild type conditions. C. NICD GoF, apoptosis is no longer reachable. D. p53 LoF and NICD GoF, only metastasis is observed. Note that HS stands for "Homeostatic State" and CCA for "CellCycleArrest."

doi:10.1371/journal.pcbi.1004571.g003

The probabilities of the four phenotypes for wild type conditions are shown in Fig 3A. They show all possible phenotypes for all input configurations. Note that *Metastasis* can be only reached in the wild type for a particular set of initial conditions (ECMicroenv, GF and TGFbeta all ON), which might correspond to extreme situations. The mutant p53 LoF is very similar to the wild type in terms of possible phenotypes (Fig 2A). The NICD GoF mutation, compared to the wild type, showed an increased probability for EMT as previously reported [126]. *Metastasis* could be reached as well in this single mutant with a higher probability than in the wild type; *Apoptosis* is no longer reachable, confirming that Notch pathway is a pro-survival pathway (Figs 2A and 3C). In addition, in this mutant, *Metastasis* was clearly blocked by p53 since a loss of function of p53 in a NICD GoF mutant completely suppressed both the *EMT* and

Invasion phenotypes present in the single mutant, and only *Metastasis* could be reached (Fig 3D). The deletion of both p63 and p73 in a NICD GOF mutant maintained the *EMT* phenotype (not shown) proving the importance of p53 in protecting the cells from metastasis.

In this context, we further investigated the role of TGF-β pathway in metastasis. Although the NICD GoF/p53 LoF double mutation has been predicted to be the best mutation to acquire metastasis, an important role for the TGF-β pathway is suggested by the model. The triple mutant NICD GoF, p53 LoF and TGF-β LoF (S4 Table) seems to suppress the metastatic process in the model: cells are able to go through EMT but cannot invade the tissue. Suppressing the TGF-β pathway might be an interesting therapeutic option to control metastasis in patients; however more studies are required to test this hypothesis.

Discussion

In this study, we propose a logical model focusing on the specific conditions that could allow the occurrence of metastasis. Our model of the metastatic process represents its early steps: EMT, invasion and migration. A cell acquires the capability to migrate when both EMT and invasion abilities have been acquired. These steps are regulated by several signalling pathways, where genetic aberrations could influence the efficiency of metastatic process. Both the influence network and the assignment of logical rules for each node of this network have been derived from what has been published from experimental works as of today. With this model, we were able to explore known conditions (and predict new ones) required for the occurrence of metastasis. Our influence network describes the regulation of EMT, invasion, migration, cell cycle arrest and apoptosis known from the literature. In this regulatory network, cell cycle arrest and apoptosis are mechanisms or phenotypes that maintain homeostasis of organs [127] or ways to evade metastasis. Cell migration depends on pathways involving AKT, ERK, Vimentin, miR200 and p63 but also on the acquisition of EMT and invasive abilities such as producing MMPs to dissolve the *laminae propria* enabling migration to distant sites. Cells that have only invasive properties are not able to move as they are still well attached to their surrounding neighbouring cells resulting in absence of cell migration. Only when those two requirements are met and the other pathways allow migration, can metastasis occur.

The role of each EMT regulator, for acquiring invasive properties, has been investigated and the model shows that each individual EMT regulator is sufficient to induce EMT when overexpressed and with the appropriate initial conditions. The model also predicts that a LoF mutation of the EMT regulators does not affect metastasis except for ZEB2 and TWIST1: ZEB2 inhibition leads to abrogation of migration, while a TWIST1 LoF leads to inhibition of EMT, since TWIST1 is the only transcription factor that can induce transcription of *cdh2* gene which is required to have EMT. These regulators are interesting targets for therapy since both are more downstream in the metastasis' cascade knowing that most activating mutations occur relatively more upstream e.g. KRAS and EGFR mutations.

The model has been validated using experimental data by matching the transcriptomic data with stable state solutions of the logical model. The direct comparison between stable states and gene expression of tumour samples shows no conclusive results. This may be due to that only at the front of tumours, cells undergo EMT and this signal is obscured by the bulk of the tumour [30,128]. On the other hand, the model matches well the transcriptomic data from a time course experiment of lung carcinoma cell lines in which EMT was induced by increasing concentration of TGF-β.

Qualitative simulations of the model using MaBoSS confirmed that single mutations are not sufficient to enable metastasis. Therefore, we systematically computed the level of epistasis of each two-gene mutation with respect to reaching the metastatic phenotype. We determined

which double mutations are the most efficient for inducing metastasis with NICD GoF/p53 LoF mutations being the most efficient combination of gene knock-out and over-dosage, as this double mutant leads *in silico* to 100% probability of having metastasis.

In our previous work, this specific double mutation NICD GoF/p53 LoF has been carried out experimentally in a mouse model, by crossing the *villin-CreERT2* mice [129] (in this study referred as p53 LoF) and *RosaN1ic* mice [130] (in this study referred as NICD GoF) with the isogenic C57BL/6 animals to generate the NICD GoF/p53 LoF compound mice. These compound mice develop intestinal tumours with metastatic tumours to distal organs [31]. Our logical model successfully reproduces experimental observations of the compound mouse and proposes mechanisms explaining the metastatic phenotype with high penetrance in mice. In addition, we have investigated the role of TGF-β pathway in metastasis and showed its crucial role in the metastatic phenotype in the double mutant. Suppressing the TGF-β pathway might be an interesting target therapy to control metastasis, however future studies are required.

We also explored the activity of the Wnt pathway in the double mutant. Increased activity of the Wnt pathway due to mutations in the *apc* and *ctnnb1* genes leads to tumourigenesis of many cancers [131–133] and subsequently to metastasis [134,135]. Our mathematical model predicts phenotypes that correspond to adenocarcinomas as a result of linear progression of acquired mutations during sporadic colorectal cancer (CRC) suggested by the "Vogelstein sequence" [136] but no metastasis is reached with the model. Indeed, when we simulate APC LoF, KRAS GoF and p53 LoF (the Vogelstein sequence), the model predicts stable states of cells that are not arrested in the cell cycle, can undergo EMT and can invade (see S4 Table). Thus our logical model supports the hypothesis that the Wnt pathway contributes to tumour initiation [137]. However, there is still a debate if the Wnt pathway is actively involved in metastasis. For example, a negative correlation has been demonstrated between the presence of β-catenin and metastasis in breast cancer [138], in lung cancer [139–141], and in CRC [142–144]. It has been also demonstrated that the canonical Wnt pathway (β-catenin-dependent pathway) is suppressed at the leading edge of the tumour [145] and this might happen without affecting the β-catenin protein levels [146,147]. In the mouse model with Notch GoF /p53 LoF double mutation, in some tumours samples, mutations in *apc* and *ctnnb1* have been found but also tumours without those mutations have been shown to acquire metastasis. Both truncated APC and mutations in β-catenin correspond in our mathematical model to full activation of CTNNB1 and this will induce activation of AKT1. In our model, activation of AKT1 will inhibit migration and therefore inhibit metastasis. Appearance of metastasis in the mouse model with activated Wnt pathway might be putatively explained if one looks at the length of the truncated APC isoform for tumours with *apc* mutation. The APC mutation found in the Notch GoF /p53 LoF mouse model results in a relatively large truncated APC isoform that might still have inhibitory effect on β-catenin [148]. More details about the APC isoforms and its effect on β-catenin can be found in S3 Text.

Another explanation for having metastasis in tumours with active Wnt pathway might be the involvement of another mutation that affects the *akt1* or the *akt2* gene. According to our model, the Wnt pathway inhibits metastasis by up-regulation of AKT1. There are tumours in CRC patients (TCGA data from http://cbioportal.org, [31]) that can have an *akt2* gene amplification or a homozygous deletion or missense mutation of *akt1*. AKT2 induces migration while AKT1 inhibits migration thus the ratio AKT1 to AKT2 might be an important determinant for acquiring metastasis in the colon. Indeed studies have shown that AKT2 is predominant in sporadic colon cancer [149] and have a critical role in metastasis in CRC [150].

A Boolean model of EMT induction has been recently published, where the theoretical prediction that the Wnt pathway can be activated upon TGF-β administration was validated experimentally by measuring increased gene expression of the Wnt target gene *axin2* in Huh7

and PLC/PRF/5 cell lines [151]. Those cell lines are derived from hepatocellular carcinomas [152,153] and both can harbour known mutations [154] and unconfirmed mutations (http://tinyurl.com/l6mjd8y) that affect the signalling pathways: the Wnt pathway has constitutive activity in the Huh7 cell line [137,155]. An alternative explanation could be that our model is more specific for epithelial cancers as the model depicts many reactions observed in epithelial cells; it has been shown that different types of cancer have different protein (or isoforms) abundance [112,149]. Therefore, our model might be less adequate in predicting the activity for certain nodes for hepatocellular carcinoma and lung adenocarcinoma.

EMT is considered to be the first step and is very often modelled as an equivalent of having metastasis once it is activated. We provide here a logical model that proposes the involvement of three independent processes in order to have metastasis: EMT, invasion and migration. These phenotypes are controlled by an intricate network and only when EMT, invasion and migration do occur, can metastasis happen. The logical model explores the mechanisms and interplays between pathways that are involved in the processes, identifies the main players in these mechanisms and gives insight on how these pathways could be altered in a therapeutic perspective. Note that other mechanisms involving other alterations in the pathways that we model, or in other pathways might also take place, and we do not claim that our approach cover all possibilities of inducing metastasis. Still, our approach provides candidate intervention points for designing innovative anti-metastatic strategies.

Supporting Information

S1 Text. Review on published articles of mathematical models of EMT.
(DOCX)

S2 Text. Link between model solutions and transcriptomics data.
(DOCX)

S3 Text. Description of Wnt pathway.
(PDF)

S4 Text. From the master model to the reduced model.
(DOCX)

S1 Fig. Colon transcriptomics data. Mean value expression for each gene is mapped on the network. The figure is the same for both metastatic and non-metastatic samples.
(PNG)

S2 Fig. Modular network of the metastasis model.
(PDF)

S3 Fig. Colon transcriptomics data mapped onto the modular network. The score for the modules are calculated based on the expression of target genes for metastatic and non-metastatic samples.
(PDF)

S4 Fig. Mean gene expression value of the three replicates for the genes of the network at 4 different time points: At t = 0, at t = 8h, at t = 24h and at t = 72h. Green nodes correspond to low expression and red nodes to high expression. The minimum and maximum expression values are set over the whole dataset and are the same for the four graphs.
(PDF)

S5 Fig. Distribution of pairs of genes of the mathematical model in the four-dimensional space of *Metastasis* probabilities, corresponding to four possible mutation type

combinations **LoF/LoF, LoF/GoF, GoF/LoF, GoF/GoF (here LoF is Loss-of-Function and GoF is Gain-of-Function).** The image shows a two-dimensional projection onto a non-linear principal manifold from the space defined by four metastatic phenotype probabilities [p(LoF/LoF);p(GoF/GoF); p(LoF/GoF)+p(GoF/LoF);|p(LoF/GoF)-p(GoF/LoF)|]. Projection density is shown in the background by grey shading. The size of the node corresponds to the amplitude of the node pair (maximum difference in phenotype probability between the four mutants: LoF/LoF, GoF/GoF, GoF/LoF, LoF/GoF), such that the most sensitive (allowing control of phenotype to maximal degree) gene pairs correspond to bigger node sizes. Five clusters are identified: they correspond to five patterns which existence can be guessed from the symmetry considerations and which are shown on the right panels. 1a) Any GoF cancels the phenotype while double LoF can amplify it (14% of gene pairs); 1b) Any LoF cancels the phenotype while double GoF can amplify it (13%); 2a) Double GoF cancels the phenotype, double LoF or synthetic-dosage interaction can amplify it (23%); 2b) Double LoF cancels the phenotype, double GoF or synthetic-dosage interaction (LoF/GoF or GoF/LoF) can amplify it (16%); 3) Double LoF and double GoF cancel the phenotype, while synthetic-dosage interaction can amplify it (30%). TP53-NICD (top-left corner) mutant is an extreme example of group 3. NICD-AKT2 (bottom-left corner) is an extreme example of group 2b.
(PNG)

S6 Fig. Results of robustness tests for the logical model with respect to small changes in the logical rules of the model. In the wild type logical model, for each logical rule, several "variant" models were created by changing one or two "OR" or "AND" operators to "AND" or "OR" operators respectively. The resulting distributions of phenotype probabilities over all such model modifications are shown.
(PDF)

S1 Table. Annotations of the logical model.
(DOCX)

S2 Table. Phenotypes that can be reached by setting the activity of a single module or pathway to always ON (GoF: gain of function) or always OFF (LoF: loss of function).
(XLSX)

S3 Table. Phenotypes that can be reached by setting the activity of a single EMT regulator to always ON (GoF: gain of function) or always OFF (LoF: loss of function). EMT regulators: Snai1, Snai2, Zeb1, Zeb2, and Twist1.
(XLSX)

S4 Table. Table of mutants. For each condition or mutation, all possible inputs are considered. Thus, all possible outputs corresponding to stable states are shown in this table (values for internal variables are not shown). The existence of a stable state in accordance with what has been published is enough to conclude that the mutant is validated: there exists a condition for which the model explains the experiments. The fact that other stable states exist shows that for some particular conditions, the stable state could be reachable. For instance, for NICD GoF, we see that a stable state with metastasis exits which has not been observed in experiments. However, for this stable state, all p53 family members are OFF, thus, it is a particular situation.
(DOCX)

S5 Table. Signatures of module activity.
(XLS)

S6 Table. Robustness analysis; table of mutants for the logical stable states of the perturbed models.
(XLSX)

S1 File. Detailed and modular models in GINsim and MaBoSS formats. The zip file includes: Detailed model in GINsim format (SuppMat_Model_Master_Model.zginml), Modular model in GINsim format (SuppMat_Model_ModNet.zginml), SuppMat_MaBoSS_Master-Model.bnd (To simulate the model, MaBoSS needs to be downloaded from maboss.curie.fr and launched with the following command line:./MaBoSS -c SuppMat_MaBoSS_MasterModel.cfg -o SuppMat_MaBoSS_MasterModel SuppMat_MaBoSS_MasterModel.bnd), SuppMat_Ma-BoSS_MasterModel.cfg, SuppMat_MaBoSS_ModNet.bnd (To simulate the model, MaBoSS needs to be downloaded from maboss.curie.fr and launched with the following command line:./MaBoSS -c SuppMat_MaBoSS_ModNet.cfg -o SuppMat_MaBoSS_ModNet SuppMat_MaBoSS_ModNet.bnd), SuppMat_MaBoSS_ModNet.cfg.
(ZIP)

S2 File. SuppMat_metastasis_mutants.cys.
(ZIP)

Acknowledgments

We are thankful to Prof Dr Daniel Louvard for critical reading and advising on the manuscript.

Author Contributions

Conceived and designed the experiments: DPAC LM SR EB AZ LC. Performed the experiments: DPAC LM AZ LC. Analyzed the data: LM DPAC AZ LC. Contributed reagents/materials/analysis tools: DPAC LM AZ LC. Wrote the paper: DPAC LM AZ EB LC. Contributed to the model construction: DPAC SR EB AZ LC. Corrected the manuscript: SR EB.

References

1. Siegel R, Ward E, Brawley O, Jemal A Cancer statistics, 2011: the impact of eliminating socioeconomic and racial disparities on premature cancer deaths. CA Cancer J Clin 61: 212–236. doi: 10.3322/caac.20121 PMID: 21685461

2. Reymond N, D'Água BB, Ridley AJ (2013) Crossing the endothelial barrier during metastasis. Nat Rev Cancer 13: 858–870. doi: 10.1038/nrc3628 PMID: 24263189

3. Van Zijl F, Krupitza G, Mikulits W (2011) Initial steps of metastasis: cell invasion and endothelial transmigration. Mutat Res 728: 23–34. doi: 10.1016/j.mrrev.2011.05.002 PMID: 21605699

4. Ramaswamy S, Ross KN, Lander ES, Golub TR (2003) A molecular signature of metastasis in primary solid tumors. Nat Genet 33: 49–54. doi: 10.1038/ng1060 PMID: 12469122

5. Podsypanina K, Du Y-CN, Jechlinger M, Beverly LJ, Hambardzumyan D, et al. (2008) Seeding and propagation of untransformed mouse mammary cells in the lung. Science 321: 1841–1844. doi: 10.1126/science.1161621 PMID: 18755941

6. Conteduca V, Zamarchi R, Rossi E, Condelli V, Troiani L, et al. (2013) Circulating tumor cells: utopia or reality? Future Oncol 9: 1337–1352. doi: 10.2217/fon.13.101 PMID: 23980681

7. Thiery JP, Acloque H, Huang RYJ, Nieto MA (2009) Epithelial-mesenchymal transitions in development and disease. Cell 139: 871–890. doi: 10.1016/j.cell.2009.11.007 PMID: 19945376

8. Foroni C, Broggini M, Generali D, Damia G (2012) Epithelial-mesenchymal transition and breast cancer: Role, molecular mechanisms and clinical impact. Cancer Treat Rev 38: 689–697. doi: 10.1016/j.ctrv.2011.11.001 PMID: 22118888

9. Kalluri R, Weinberg RA (2009) The basics of epithelial-mesenchymal transition. J Clin Invest 119: 1420–1428. doi: 10.1172/JCI39104 PMID: 19487818

10. Zeisberg M, Neilson EG (2009) Biomarkers for epithelial-mesenchymal transitions. J Clin Invest 119: 1429–1437. doi: 10.1172/JCI36183 PMID: 19487819

11. Sánchez-Tilló E, Liu Y, de Barrios O, Siles L, Fanlo L, et al. (2012) EMT-activating transcription factors in cancer: beyond EMT and tumor invasiveness. Cell Mol Life Sci 69: 3429–3456. doi: 10.1007/s00018-012-1122-2 PMID: 22945800

12. Nieto MA (2011) The ins and outs of the epithelial to mesenchymal transition in health and disease. Annu Rev Cell Dev Biol 27: 347–376. doi: 10.1146/annurev-cellbio-092910-154036 PMID: 21740232

13. Geiger TR, Peeper DS (2009) Metastasis mechanisms. Biochim Biophys Acta 1796: 293–308. doi: 10.1016/j.bbcan.2009.07.006 PMID: 19683560

14. Polyak K, Weinberg RA (2009) Transitions between epithelial and mesenchymal states: acquisition of malignant and stem cell traits. Nat Rev Cancer 9: 265–273. doi: 10.1038/nrc2620 PMID: 19262571

15. Thiery JP, Sleeman JP (2006) Complex networks orchestrate epithelial-mesenchymal transitions. Nat Rev Mol Cell Biol 7: 131–142. doi: 10.1038/nrm1835 PMID: 16493418

16. Wang S-P, Wang W-L, Chang Y-L, Wu C-T, Chao Y-C, et al. (2009) p53 controls cancer cell invasion by inducing the MDM2-mediated degradation of Slug. Nat Cell Biol 11: 694–704. doi: 10.1038/ncb1875 PMID: 19448627

17. Jonkers J, Meuwissen R, van der Gulden H, Peterse H, van der Valk M, et al. (2001) Synergistic tumor suppressor activity of BRCA2 and p53 in a conditional mouse model for breast cancer. Nat Genet 29: 418–425. doi: 10.1038/ng747 PMID: 11694875

18. Wijnhoven BP, Dinjens WN, Pignatelli M (2000) E-cadherin-catenin cell-cell adhesion complex and human cancer. Br J Surg 87: 992–1005. doi: 10.1046/j.1365-2168.2000.01513.x PMID: 10931041

19. Le Bras GF, Taubenslag KJ, Andl CD (2012) The regulation of cell-cell adhesion during epithelial-mesenchymal transition, motility and tumor progression. Cell Adh Migr 6: 365–373. doi: 10.4161/cam.21326 PMID: 22796940

20. Bravo-Cordero JJ, Hodgson L, Condeelis J (2012) Directed cell invasion and migration during metastasis. Curr Opin Cell Biol 24: 277–283. doi: 10.1016/j.ceb.2011.12.004 PMID: 22209238

21. Wan L, Pantel K, Kang Y (2013) Tumor metastasis: moving new biological insights into the clinic. Nat Med 19: 1450–1464. doi: 10.1038/nm.3391 PMID: 24202397

22. Bauvois B (2012) New facets of matrix metalloproteinases MMP-2 and MMP-9 as cell surface transducers: outside-in signaling and relationship to tumor progression. Biochim Biophys Acta 1825: 29–36. doi: 10.1016/j.bbcan.2011.10.001 PMID: 22020293

23. Barillot E, Calzone L, Hupé P, Vert J-P, Zinovyev A (2012) Computational Systems Biology of Cancer. Chapman & Hall/CRC. 461 p.

24. Anderson ARA, Weaver AM, Cummings PT, Quaranta V (2006) Tumor morphology and phenotypic evolution driven by selective pressure from the microenvironment. Cell 127: 905–915. doi: 10.1016/j.cell.2006.09.042 PMID: 17129778

25. Martin NK, Gaffney EA, Gatenby RA, Maini PK (2010) Tumour-stromal interactions in acid-mediated invasion: a mathematical model. J Theor Biol 267: 461–470. doi: 10.1016/j.jtbi.2010.08.028 PMID: 20816684

26. Knutsdottir H, Palsson E, Edelstein-Keshet L (2014) Mathematical model of macrophage-facilitated breast cancer cells invasion. J Theor Biol. doi: 10.1016/j.jtbi.2014.04.031

27. Lu M, Jolly MK, Levine H, Onuchic JN, Ben-Jacob E (2013) MicroRNA-based regulation of epithelial-hybrid-mesenchymal fate determination. Proc Natl Acad Sci U S A 110: 18144–18149. doi: 10.1073/pnas.1318192110 PMID: 24154725

28. Tian X-J, Zhang H, Xing J (2013) Coupled reversible and irreversible bistable switches underlying TGFβ-induced epithelial to mesenchymal transition. Biophys J 105: 1079–1089. doi: 10.1016/j.bpj.2013.07.011 PMID: 23972859

29. Zhang J, Tian X-J, Zhang H, Teng Y, Li R, et al. (2014) TGF-β-induced epithelial-to-mesenchymal transition proceeds through stepwise activation of multiple feedback loops. Sci Signal 7: ra91. doi: 10.1126/scisignal.2005304

30. Sethi S, Macoska J, Chen W, Sarkar FH (2010) Molecular signature of epithelial-mesenchymal transition (EMT) in human prostate cancer bone metastasis. Am J Transl Res 3: 90–99. PMID: 21139809

31. Chanrion M, Kuperstein I, Barrière C, El Marjou F, Cohen D, et al. (2014) Concomitant Notch activation and p53 deletion trigger epithelial-to-mesenchymal transition and metastasis in mouse gut. Nat Commun 5: 5005. doi: 10.1038/ncomms6005 PMID: 25295490

32. Tsai JH, Yang J (2013) Epithelial-mesenchymal plasticity in carcinoma metastasis. Genes Dev 27: 2192–2206. doi: 10.1101/gad.225334.113 PMID: 24142872

33. Signaling network of EMT regulation http://navicell.curie.fr/navicell/maps/signallingnetworkofemtregulation/master/index.html

34. Kim Y-N, Koo KH, Sung JY, Yun U-J, Kim H (2012) Anoikis resistance: an essential prerequisite for tumor metastasis. Int J Cell Biol 2012: 306879. doi: 10.1155/2012/306879 PMID: 22505926

35. Subramanian A, Tamayo P, Mootha VK, Mukherjee S, Ebert BL, et al. (2005) Gene set enrichment analysis: a knowledge-based approach for interpreting genome-wide expression profiles. Proc Natl Acad Sci U S A 102: 15545–15550. doi: 10.1073/pnas.0506580102 PMID: 16199517

36. Bild AH, Yao G, Chang JT, Wang Q, Potti A, et al. (2006) Oncogenic pathway signatures in human cancers as a guide to targeted therapies. Nature 439: 353–357. doi: 10.1038/nature04296 PMID: 16273092

37. Kanehisa M, Goto S, Kawashima S, Okuno Y, Hattori M (2004) The KEGG resource for deciphering the genome. Nucleic Acids Res 32: D277–D280. doi: 10.1093/nar/gkh063 PMID: 14681412

38. The Henome Cancer Atlas Network (2012) Comprehensive molecular characterization of human colon and rectal cancer. Nature 487: 330–337. doi: 10.1038/nature11252 PMID: 22810696

39. Sartor MA, Mahavisno V, Keshamouni VG, Cavalcoli J, Wright Z, et al. (2010) ConceptGen: a gene set enrichment and gene set relation mapping tool. Bioinformatics 26: 456–463. doi: 10.1093/bioinformatics/btp683 PMID: 20007254

40. Qin H, Chan MWY, Liyanarachchi S, Balch C, Potter D, et al. (2009) An integrative ChIP-chip and gene expression profiling to model SMAD regulatory modules. BMC Syst Biol 3: 73. doi: 10.1186/1752-0509-3-73 PMID: 19615063

41. Müssel C, Hopfensitz M, Kestler HA (2010) BoolNet—an R package for generation, reconstruction and analysis of Boolean networks. Bioinformatics 26: 1378–1380. doi: 10.1093/bioinformatics/btq124 PMID: 20378558

42. Gorban A, Kegl B, Wunch D, Zinovyev A, editors (2008) Principal Manifolds for Data Visualisation and Dimension Reduction. Vol. 58. Berlin-Heidelberg: Springer. 340 p.

43. Gorban AN, Zinovyev A (2010) Principal manifolds and graphs in practice: from molecular biology to dynamical systems. Int J Neural Syst 20: 219–232. doi: 10.1142/S0129065710002383 PMID: 20556849

44. Gorban A., Pitenko A., Zinovyev A (2014) ViDaExpert: user-friendly tool for nonlinear visualization and analysis of multidimensional vectorial data. URL: http://arxiv.org/abs/1406.5550

45. Drasin DJ, Robin TP, Ford HL (2011) Breast cancer epithelial-to-mesenchymal transition: examining the functional consequences of plasticity. Breast Cancer Res 13: 226. doi: 10.1186/bcr3037 PMID: 22078097

46. Moreno-Bueno G, Cubillo E, Sarrió D, Peinado H, Rodríguez-Pinilla SM, et al. (2006) Genetic profiling of epithelial cells expressing E-cadherin repressors reveals a distinct role for Snail, Slug, and E47 factors in epithelial-mesenchymal transition. Cancer Res 66: 9543–9556. doi: 10.1158/0008-5472.CAN-06-0479 PMID: 17018611

47. Conacci-Sorrell M, Simcha I, Ben-Yedidia T, Blechman J, Savagner P, et al. (2003) Autoregulation of E-cadherin expression by cadherin-cadherin interactions: the roles of beta-catenin signaling, Slug, and MAPK. J Cell Biol 163: 847–857. doi: 10.1083/jcb.200308162 PMID: 14623871

48. Yang J, Mani SA, Donaher JL, Ramaswamy S, Itzykson RA, et al. (2004) Twist, a master regulator of morphogenesis, plays an essential role in tumor metastasis. Cell 117: 927–939. doi: 10.1016/j.cell.2004.06.006 PMID: 15210113

49. Liu Y, El-Naggar S, Darling DS, Higashi Y, Dean DC (2008) Zeb1 links epithelial-mesenchymal transition and cellular senescence. Development 135: 579–588. doi: 10.1242/dev.007047 PMID: 18192284

50. Comijn J, Berx G, Vermassen P, Verschueren K, van Grunsven L, et al. (2001) The two-handed E box binding zinc finger protein SIP1 downregulates E-cadherin and induces invasion. Mol Cell 7: 1267–1278. PMID: 11430829

51. Katsuno Y, Lamouille S, Derynck R (2013) TGF-β signaling and epithelial-mesenchymal transition in cancer progression. Curr Opin Oncol 25: 76–84. PMID: 23197193

52. Mao Y, Xu J, Li Z, Zhang N, Yin H, et al. (2013) The role of nuclear β-catenin accumulation in the Twist2-induced ovarian cancer EMT. PLoS One 8: e78200. doi: 10.1371/journal.pone.0078200 PMID: 24244294

53. Espinoza I, Miele L (2013) Deadly crosstalk: Notch signaling at the intersection of EMT and cancer stem cells. Cancer Lett. doi: 10.1016/j.canlet.2013.08.027

54. Timmerman LA, Grego-Bessa J, Raya A, Bertrán E, Pérez-Pomares JM, et al. (2004) Notch promotes epithelial-mesenchymal transition during cardiac development and oncogenic transformation. Genes Dev 18: 99–115. doi: 10.1101/gad.276304 PMID: 14701881

55. Grille SJ, Bellacosa A, Upson J, Klein-Szanto AJ, van Roy F, et al. (2003) The protein kinase Akt induces epithelial mesenchymal transition and promotes enhanced motility and invasiveness of squamous cell carcinoma lines. Cancer Res 63: 2172–2178. PMID: 12727836

56. Suman S, Kurisetty V, Das TP, Vadodkar A, Ramos G, et al. (2013) Activation of AKT signaling promotes epithelial-mesenchymal transition and tumor growth in colorectal cancer cells. Mol Carcinog. doi: 10.1002/mc.22076

57. Hill L, Browne G, Tulchinsky E (2012) ZEB/miR-200 feedback loop: At the crossroads of signal transduction in cancer. Int J Cancer. doi: 10.1002/ijc.27708

58. Liu Y-N, Yin JJ, Abou-Kheir W, Hynes PG, Casey OM, et al. (2012) MiR-1 and miR-200 inhibit EMT via Slug-dependent and tumorigenesis via Slug-independent mechanisms. Oncogene. doi: 10.1038/onc.2012.58

59. Moes M, Le Béchec A, Crespo I, Laurini C, Halavatyi A, et al. (2012) A Novel Network Integrating a miRNA-203/SNAI1 Feedback Loop which Regulates Epithelial to Mesenchymal Transition. PLoS One 7: e35440. doi: 10.1371/journal.pone.0035440 PMID: 22514743

60. Siemens H, Jackstadt R, Hünten S, Kaller M, Menssen A, et al. (2011) miR-34 and SNAIL form a double-negative feedback loop to regulate epithelial-mesenchymal transitions. Cell Cycle 10: 4256–4271. doi: 10.4161/cc.10.24.18552 PMID: 22134354

61. Hao L, Ha JR, Kuzel P, Garcia E, Persad S (2012) Cadherin switch from E- to N-cadherin in melanoma progression is regulated by the PI3K/PTEN pathway through Twist and Snail. Br J Dermatol 166: 1184–1197. doi: 10.1111/j.1365-2133.2012.10824.x PMID: 22332917

62. McKenna DJ, McDade SS, Patel D, McCance DJ (2010) MicroRNA 203 expression in keratinocytes is dependent on regulation of p53 levels by E6. J Virol 84: 10644–10652. doi: 10.1128/JVI.00703-10 PMID: 20702634

63. Tarasov V, Jung P, Verdoodt B, Lodygin D, Epanchintsev A, et al. (2007) Differential regulation of microRNAs by p53 revealed by massively parallel sequencing: miR-34a is a p53 target that induces apoptosis and G1-arrest. Cell Cycle 6: 1586–1593. PMID: 17554199

64. Kim NH, Kim HS, Li X-Y, Lee I, Choi H-S, et al. (2011) A p53/miRNA-34 axis regulates Snail1-dependent cancer cell epithelial-mesenchymal transition. J Cell Biol 195: 417–433. doi: 10.1083/jcb.201103097 PMID: 22024162

65. Knouf EC, Garg K, Arroyo JD, Correa Y, Sarkar D, et al. (2012) An integrative genomic approach identifies p73 and p63 as activators of miR-200 microRNA family transcription. Nucleic Acids Res 40: 499–510. doi: 10.1093/nar/gkr731 PMID: 21917857

66. Antonini D, Russo MT, De Rosa L, Gorrese M, Del Vecchio L, et al. (2010) Transcriptional repression of miR-34 family contributes to p63-mediated cell cycle progression in epidermal cells. J Invest Dermatol 130: 1249–1257. doi: 10.1038/jid.2009.438 PMID: 20090763

67. Agostini M, Tucci P, Steinert JR, Shalom-Feuerstein R, Rouleau M, et al. (2011) microRNA-34a regulates neurite outgrowth, spinal morphology, and function. Proc Natl Acad Sci U S A 108: 21099–21104. doi: 10.1073/pnas.1112063108 PMID: 22160706

68. Saini S, Majid S, Yamamura S, Tabatabai L, Suh SO, et al. (2011) Regulatory Role of mir-203 in Prostate Cancer Progression and Metastasis. Clin Cancer Res 17: 5287–5298. doi: 10.1158/1078-0432.CCR-10-2619 PMID: 21159887

69. Blandino G, Dobbelstein M (2004) p73 and p63: why do we still need them? Cell Cycle 3: 886–894. PMID: 15254416

70. Dötsch V, Bernassola F, Coutandin D, Candi E, Melino G (2010) p63 and p73, the ancestors of p53. Cold Spring Harb Perspect Biol 2: a004887. doi: 10.1101/cshperspect.a004887 PMID: 20484388

71. Allocati N, Di Ilio C, De Laurenzi V (2012) p63/p73 in the control of cell cycle and cell death. Exp Cell Res 318: 1285–1290. doi: 10.1016/j.yexcr.2012.01.023 PMID: 22326462

72. Dotto GP (2009) Crosstalk of Notch with p53 and p63 in cancer growth control. Nat Rev Cancer 9: 587–595. doi: 10.1038/nrc2675 PMID: 19609265

73. Moro L, Arbini AA, Yao JL, di Sant'Agnese PA, Marra E, et al. (2009) Mitochondrial DNA depletion in prostate epithelial cells promotes anoikis resistance and invasion through activation of PI3/Akt2. Cell Death Differ 16: 571–583. doi: 10.1038/cdd.2008.178 PMID: 19079138

74. Forster N, Ellisen LW (2011) Notch signaling mediates p63-induced quiescence: a new facet of p63/Notch crosstalk. Cell Cycle 10: 3632–3633. doi: 10.4161/cc.10.21.18182 PMID: 22041817

75. Zdzalik M, Pustelny K, Kedracka-Krok S, Huben K, Pecak A, et al. (2010) Interaction of regulators Mdm2 and Mdmx with transcription factors p53, p63 and p73. Cell Cycle 9: 4584–4591. PMID: 21088494

76. Feng Z, Levine AJ (2010) The regulation of energy metabolism and the IGF-1/mTOR pathways by the p53 protein. Trends Cell Biol 20: 427–434. doi: 10.1016/j.tcb.2010.03.004 PMID: 20399660

77. Kubo N, Okoshi R, Nakashima K, Shimozato O, Nakagawara A, et al. (2010) MDM2 promotes the proteasomal degradation of p73 through the interaction with Itch in HeLa cells. Biochem Biophys Res Commun 403: 405–411. doi: 10.1016/j.bbrc.2010.11.043 PMID: 21093410

78. Zhang X, Tang N, Hadden TJ, Rishi AK (2011) Akt, FoxO and regulation of apoptosis. Biochim Biophys Acta 1813: 1978–1986. doi: 10.1016/j.bbamcr.2011.03.010 PMID: 21440011

79. Xu J, Zhou J-Y, Wei W-Z, Wu GS (2010) Activation of the Akt survival pathway contributes to TRAIL resistance in cancer cells. PLoS One 5: e10226. doi: 10.1371/journal.pone.0010226 PMID: 20419107

80. Li Y, Dowbenko D, Lasky LA (2002) AKT/PKB phosphorylation of p21Cip/WAF1 enhances protein stability of p21Cip/WAF1 and promotes cell survival. J Biol Chem 277: 11352–11361. doi: 10.1074/jbc.M109062200 PMID: 11756412

81. Iliopoulos D, Polytarchou C, Hatziapostolou M, Kottakis F, Maroulakou IG, et al. (2009) MicroRNAs differentially regulated by Akt isoforms control EMT and stem cell renewal in cancer cells. Sci Signal 2: ra62. doi: 10.1126/scisignal.2000356 PMID: 19825827

82. Chin YR, Toker A (2010) The actin-bundling protein palladin is an Akt1-specific substrate that regulates breast cancer cell migration. Mol Cell 38: 333–344. doi: 10.1016/j.molcel.2010.02.031 PMID: 20471940

83. Chin YR, Toker A (2011) Akt isoform-specific signaling in breast cancer: uncovering an anti-migratory role for palladin. Cell Adh Migr 5: 211–214. PMID: 21519185

84. Liu H, Radisky DC, Nelson CM, Zhang H, Fata JE, et al. (2006) Mechanism of Akt1 inhibition of breast cancer cell invasion reveals a protumorigenic role for TSC2. Proc Natl Acad Sci U S A 103: 4134–4139. doi: 10.1073/pnas.0511342103 PMID: 16537497

85. Héron-Milhavet L, Franckhauser C, Rana V, Berthenet C, Fisher D, et al. (2006) Only Akt1 is required for proliferation, while Akt2 promotes cell cycle exit through p21 binding. Mol Cell Biol 26: 8267–8280. doi: 10.1128/MCB.00201-06 PMID: 16982699

86. Heron-Milhavet L, Franckhauser C, Fernandez A, Lamb NJ (2013) Characterization of the Akt2 domain essential for binding nuclear p21cip1 to promote cell cycle arrest during myogenic differentiation. PLoS One 8: e76987. doi: 10.1371/journal.pone.0076987 PMID: 24194853

87. Liao Y, Hung M-C (2010) Physiological regulation of Akt activity and stability. Am J Transl Res 2: 19–42. PMID: 20182580

88. Talapatra S, Thompson CB (2001) Growth factor signaling in cell survival: implications for cancer treatment. J Pharmacol Exp Ther 298: 873–878. PMID: 11504779

89. Cabello-Verrugio C, Brandan E (2007) A novel modulatory mechanism of transforming growth factor-beta signaling through decorin and LRP-1. J Biol Chem 282: 18842–18850. doi: 10.1074/jbc.M700243200 PMID: 17485468

90. Takeuchi Y, Kodama Y, Matsumoto T (1994) Bone matrix decorin binds transforming growth factor-beta and enhances its bioactivity. J Biol Chem 269: 32634–32638. PMID: 7798269

91. Okamoto O, Fujiwara S, Abe M, Sato Y (1999) Dermatopontin interacts with transforming growth factor beta and enhances its biological activity. Biochem J 337 (Pt 3): 537–541. PMID: 9895299

92. Kopan R (2012) Notch signaling. Cold Spring Harb Perspect Biol 4. doi: 10.1101/cshperspect.a011213

93. Wu F, Stutzman A, Mo Y-Y (2007) Notch signaling and its role in breast cancer. Front Biosci 12: 4370–4383. PMID: 17485381

94. Gonzalez AG, Naldi A, Sánchez L, Thieffry D, Chaouiya C (2006) GINsim: a software suite for the qualitative modelling, simulation and analysis of regulatory networks. Biosystems 84: 91–100. doi: 10.1016/j.biosystems.2005.10.003 PMID: 16434137

95. Wang H, Wu Q, Liu Z, Luo X, Fan Y, et al. (2014) Downregulation of FAP suppresses cell proliferation and metastasis through PTEN/PI3K/AKT and Ras-ERK signaling in oral squamous cell carcinoma. Cell Death Dis 5: e1155. doi: 10.1038/cddis.2014.122 PMID: 24722280

96. Zhang L, Teng Y, Zhang Y, Liu J, Xu L, et al. (2012) C-Src-mediated RANKL-induced breast cancer cell migration by activation of the ERK and Akt pathway. Oncol Lett 3: 395–400. doi: 10.3892/ol.2011.487 PMID: 22740919

97. Zhan Y, Kim S, Izumi Y, Izumiya Y, Nakao T, et al. (2003) Role of JNK, p38, and ERK in platelet-derived growth factor-induced vascular proliferation, migration, and gene expression. Arterioscler Thromb Vasc Biol 23: 795–801. doi: 10.1161/01.ATV.0000066132.32063.F2 PMID: 12637337

98. To MD, Wong CE, Karnezis AN, Del Rosario R, Di Lauro R, et al. (2008) Kras regulatory elements and exon 4A determine mutation specificity in lung cancer. Nat Genet 40: 1240–1244. doi: 10.1038/ng.211 PMID: 18758463

99. Zhang Z, Wang Y, Vikis HG, Johnson L, Liu G, et al. (2001) Wildtype Kras2 can inhibit lung carcinogenesis in mice. Nat Genet 29: 25–33. doi: 10.1038/ng721 PMID: 11528387

100. Li H, Cao H-F, Wan J, Li Y, Zhu M-L, et al. (2007) Growth inhibitory effect of wild-type Kras2 gene on a colonic adenocarcinoma cell line. World J Gastroenterol 13: 934–938. PMID: 17352027

101. Vartanian S, Bentley C, Brauer MJ, Li L, Shirasawa S, et al. (2013) Identification of mutant K-Ras-dependent phenotypes using a panel of isogenic cell lines. J Biol Chem 288: 2403–2413. doi: 10.1074/jbc.M112.394130 PMID: 23188824

102. Benet M, Dulman RY, Suzme R, de Miera EV-S, Vega ME, et al. (2012) Wild type N-ras displays anti-malignant properties, in part by downregulating decorin. J Cell Physiol 227: 2341–2351. doi: 10.1002/jcp.22969 PMID: 21809347

103. Xu J, Haigis KM, Firestone AJ, McNerney ME, Li Q, et al. (2013) Dominant role of oncogene dosage and absence of tumor suppressor activity in Nras-driven hematopoietic transformation. Cancer Discov 3: 993–1001. doi: 10.1158/2159-8290.CD-13-0096 PMID: 23733505

104. Molinari F, Frattini M (2013) Functions and Regulation of the PTEN Gene in Colorectal Cancer. Front Oncol 3: 326. doi: 10.3389/fonc.2013.00326 PMID: 24475377

105. Aguissa-Touré A-H, Li G (2012) Genetic alterations of PTEN in human melanoma. Cell Mol Life Sci 69: 1475–1491. doi: 10.1007/s00018-011-0878-0 PMID: 22076652

106. McDowell KA, Riggins GJ, Gallia GL (2011) Targeting the AKT pathway in glioblastoma. Curr Pharm Des 17: 2411–2420. PMID: 21827416

107. Sun Z, Huang C, He J, Lamb KL, Kang X, et al. (2014) PTEN C-terminal deletion causes genomic instability and tumor development. Cell Rep 6: 844–854. doi: 10.1016/j.celrep.2014.01.030 PMID: 24561254

108. Mukherjee A, Karmakar P (2013) Attenuation of PTEN perturbs genomic stability via activation of Akt and down-regulation of Rad51 in human embryonic kidney cells. Mol Carcinog 52: 611–618. doi: 10.1002/mc.21903 PMID: 22488521

109. He L, Hou X, Kanel G, Zeng N, Galicia V, et al. (2010) The critical role of AKT2 in hepatic steatosis induced by PTEN loss. Am J Pathol 176: 2302–2308. doi: 10.2353/ajpath.2010.090931 PMID: 20348245

110. Al-Saad S, Donnem T, Al-Shibli K, Persson M, Bremnes RM, et al. (2009) Diverse prognostic roles of Akt isoforms, PTEN and PI3K in tumor epithelial cells and stromal compartment in non-small cell lung cancer. Anticancer Res 29: 4175–4183. PMID: 19846969

111. Trotman LC, Alimonti A, Scaglioni PP, Koutcher JA, Cordon-Cardo C, et al. (2006) Identification of a tumour suppressor network opposing nuclear Akt function. Nature 441: 523–527. doi: 10.1038/nature04809 PMID: 16680151

112. Chin YMR, Yuan X, Balk SP, Toker A (2014) Pten-deficient tumors depend on akt2 for maintenance and survival. Cancer Discov. doi: 10.1158/2159-8290.CD-13-0873

113. Wickremasinghe RG, Prentice AG, Steele AJ (2011) p53 and Notch signaling in chronic lymphocytic leukemia: clues to identifying novel therapeutic strategies. Leuk Off J Leuk Soc Am Leuk Res Fund, UK 25: 1400–1407. doi: 10.1038/leu.2011.103

114. Hoshino Y, Katsuno Y, Ehata S, Miyazono K (2011) Autocrine TGF-β protects breast cancer cells from apoptosis through reduction of BH3-only protein, Bim. J Biochem 149: 55–65. doi: 10.1093/jb/mvq114 PMID: 20880961

115. Xiao M, Liu YG, Zou MC, Zou F (2014) Sodium butyrate induces apoptosis of human colon cancer cells by modulating ERK and sphingosine kinase 2. Biomed Environ Sci 27: 197–203. doi: 10.3967/bes2014.040 PMID: 24709100

116. Sayan AE, Griffiths TR, Pal R, Browne GJ, Ruddick A, et al. (2009) SIP1 protein protects cells from DNA damage-induced apoptosis and has independent prognostic value in bladder cancer. Proc Natl Acad Sci U S A 106: 14884–14889. doi: 10.1073/pnas.0902042106 PMID: 19706487

117. Sahlberg SH, Gustafsson A-S, Pendekanti PN, Glimelius B, Stenerlöw B (2014) The influence of AKT isoforms on radiation sensitivity and DNA repair in colon cancer cell lines. Tumour Biol 35: 3525–3534. doi: 10.1007/s13277-013-1465-9 PMID: 24338765

118. Daroqui MC, Vazquez P, Bal de Kier Joffé E, Bakin A V, Puricelli LI (2012) TGF-β autocrine pathway and MAPK signaling promote cell invasiveness and in vivo mammary adenocarcinoma tumor progression. Oncol Rep 28: 567–575. doi: 10.3892/or.2012.1813 PMID: 22614218

119. Gomes LR, Terra LF, Wailemann RA, Labriola L, Sogayar MC (2012) TGF-β1 modulates the homeostasis between MMPs and MMP inhibitors through p38 MAPK and ERK1/2 in highly invasive breast cancer cells. BMC Cancer 12: 26. doi: 10.1186/1471-2407-12-26 PMID: 22260435

120. Tan TZ, Miow QH, Miki Y, Noda T, Mori S, et al. (2014) Epithelial-mesenchymal transition spectrum quantification and its efficacy in deciphering survival and drug responses of cancer patients. EMBO Mol Med 6: 1279–1293. doi: 10.15252/emmm.201404208 PMID: 25214461

121. Zhou H-M, Dong T-T, Wang L-L, Feng B, Zhao H-C, et al. (2012) Suppression of colorectal cancer metastasis by nigericin through inhibition of epithelial-mesenchymal transition. World J Gastroenterol 18: 2640–2648. doi: 10.3748/wjg.v18.i21.2640 PMID: 22690072

122. Wendt MK, Taylor MA, Schiemann BJ, Schiemann WP (2011) Down-regulation of epithelial cadherin is required to initiate metastatic outgrowth of breast cancer. Mol Biol Cell 22: 2423–2435. doi: 10.1091/mbc.E11-04-0306 PMID: 21613543

123. Stoll G, Viara E, Barillot E, Calzone L (2012) Continuous time Boolean modeling for biological signaling: application of Gillespie algorithm. BMC Syst Biol 6: 116. doi: 10.1186/1752-0509-6-116 PMID: 22932419

124. Muller PAJ, Vousden KH, Norman JC (2011) p53 and its mutants in tumor cell migration and invasion. J Cell Biol 192: 209–218. doi: 10.1083/jcb.201009059 PMID: 21263025

125. Wang XQ, Ongkeko WM, Lau AW, Leung KM, Poon RY (2001) A possible role of p73 on the modulation of p53 level through MDM2. Cancer Res 61: 1598–1603. PMID: 11245471

126. Wang Z, Li Y, Kong D, Banerjee S, Ahmad A, et al. (2009) Acquisition of epithelial-mesenchymal transition phenotype of gemcitabine-resistant pancreatic cancer cells is linked with activation of the notch signaling pathway. Cancer Res 69: 2400–2407. doi: 10.1158/0008-5472.CAN-08-4312 PMID: 19276344

127. Poon IKH, Lucas CD, Rossi AG, Ravichandran KS (2014) Apoptotic cell clearance: basic biology and therapeutic potential. Nat Rev Immunol 14: 166–180. doi: 10.1038/nri3607 PMID: 24481336

128. Paterson EL, Kazenwadel J, Bert AG, Khew-Goodall Y, Ruszkiewicz A, et al. (2013) Down-regulation of the miRNA-200 family at the invasive front of colorectal cancers with degraded basement membrane indicates EMT is involved in cancer progression. Neoplasia 15: 180–191. PMID: 23441132

129. El Marjou F, Janssen K-P, Chang BH-J, Li M, Hindie V, et al. (2004) Tissue-specific and inducible Cre-mediated recombination in the gut epithelium. Genesis 39: 186–193. doi: 10.1002/gene.20042 PMID: 15282745

130. Murtaugh LC, Stanger BZ, Kwan KM, Melton DA (2003) Notch signaling controls multiple steps of pancreatic differentiation. Proc Natl Acad Sci U S A 100: 14920–14925. doi: 10.1073/pnas.2436557100 PMID: 14657333

131. Herbst A, Jurinovic V, Krebs S, Thieme SE, Blum H, et al. (2014) Comprehensive analysis of β-catenin target genes in colorectal carcinoma cell lines with deregulated Wnt/β-catenin signaling. BMC Genomics 15: 74. doi: 10.1186/1471-2164-15-74 PMID: 24467841

132. Zeilstra J, Joosten SPJ, Wensveen FM, Dessing MC, Schütze DM, et al. (2011) WNT signaling controls expression of pro-apoptotic BOK and BAX in intestinal cancer. Biochem Biophys Res Commun 406: 1–6. doi: 10.1016/j.bbrc.2010.12.070 PMID: 21184732

133. Prosperi JR, Goss KH (2010) A Wnt-ow of opportunity: targeting the Wnt/beta-catenin pathway in breast cancer. Curr Drug Targets 11: 1074–1088. PMID: 20545611

134. Buda A, Pignatelli M (2011) E-cadherin and the cytoskeletal network in colorectal cancer development and metastasis. Cell Commun Adhes 18: 133–143. doi: 10.3109/15419061.2011.636465 PMID: 22176698

135. Wu K, Fan J, Zhang L, Ning Z, Zeng J, et al. (2012) PI3K/Akt to GSK3β/β-catenin signaling cascade coordinates cell colonization for bladder cancer bone metastasis through regulating ZEB1 transcription. Cell Signal 24: 2273–2282. doi: 10.1016/j.cellsig.2012.08.004 PMID: 22906492

136. Morán A, Ortega P, de Juan C, Fernández-Marcelo T, Frías C, et al. (2010) Differential colorectal carcinogenesis: Molecular basis and clinical relevance. World J Gastrointest Oncol 2: 151–158. doi: 10.4251/wjgo.v2.i3.151 PMID: 21160823

137. Yuzugullu H, Benhaj K, Ozturk N, Senturk S, Celik E, et al. (2009) Canonical Wnt signaling is antagonized by noncanonical Wnt5a in hepatocellular carcinoma cells. Mol Cancer 8: 90. doi: 10.1186/1476-4598-8-90 PMID: 19849855

138. Pang H, Lu H, Song H, Meng Q, Zhao Y, et al. (2013) Prognostic values of osteopontin-c, E-cadherin and β-catenin in breast cancer. Cancer Epidemiol 37: 985–992. doi: 10.1016/j.canep.2013.08.005 PMID: 24012693

139. Zhang H, Liu J, Yue D, Gao L, Wang D, et al. (2013) Clinical significance of E-cadherin, β-catenin, vimentin and S100A4 expression in completely resected squamous cell lung carcinoma. J Clin Pathol 66: 937–945. doi: 10.1136/jclinpath-2013-201467 PMID: 23853314

140. Chiu CG, Chan SK, Fang ZA, Masoudi H, Wood-Baker R, et al. (2012) Beta-catenin expression is prognostic of improved non-small cell lung cancer survival. Am J Surg 203: 654–659. doi: 10.1016/j.amjsurg.2012.01.002 PMID: 22402266

141. Nozawa N, Hashimoto S, Nakashima Y, Matsuo Y, Koga T, et al. (2006) Immunohistochemical alpha- and beta-catenin and E-cadherin expression and their clinicopathological significance in human lung adenocarcinoma. Pathol Res Pract 202: 639–650. doi: 10.1016/j.prp.2006.03.007 PMID: 16843618

142. Morikawa T, Kuchiba A, Yamauchi M, Meyerhardt JA, Shima K, et al. (2011) Association of CTNNB1 (beta-catenin) alterations, body mass index, and physical activity with survival in patients with colorectal cancer. JAMA 305: 1685–1694. doi: 10.1001/jama.2011.513 PMID: 21521850

143. Morikawa T, Kuchiba A, Lochhead P, Nishihara R, Yamauchi M, et al. (2013) Prospective analysis of body mass index, physical activity, and colorectal cancer risk associated with β-catenin (CTNNB1) status. Cancer Res 73: 1600–1610. doi: 10.1158/0008-5472.CAN-12-2276 PMID: 23442321

144. Bruun J, Kolberg M, Nesland JM, Svindland A, Nesbakken A, et al. (2014) Prognostic Significance of β-Catenin, E-Cadherin, and SOX9 in Colorectal Cancer: Results from a Large Population-Representative Series. Front Oncol 4: 118. doi: 10.3389/fonc.2014.00118 PMID: 24904831

145. Pourreyron C, Reilly L, Proby C, Panteleyev A, Fleming C, et al. (2012) Wnt5a is strongly expressed at the leading edge in non-melanoma skin cancer, forming active gradients, while canonical Wnt signalling is repressed. PLoS One 7: e31827. doi: 10.1371/journal.pone.0031827 PMID: 22384081

146. Mikels AJ, Nusse R (2006) Purified Wnt5a protein activates or inhibits beta-catenin-TCF signaling depending on receptor context. PLoS Biol 4: e115. doi: 10.1371/journal.pbio.0040115 PMID: 16602827

147. Yuan Y, Niu CC, Deng G, Li ZQ, Pan J, et al. (2011) The Wnt5a/Ror2 noncanonical signaling pathway inhibits canonical Wnt signaling in K562 cells. Int J Mol Med 27: 63–69. doi: 10.3892/ijmm.2010.560 PMID: 21069266

148. Wang L, Liu X, Gusev E, Wang C, Fagotto F (2014) Regulation of the phosphorylation and nuclear import and export of β-catenin by APC and its cancer-related truncated form. J Cell Sci 127: 1647–1659. doi: 10.1242/jcs.131045 PMID: 24496450

149. Roy HK, Olusola BF, Clemens DL, Karolski WJ, Ratashak A, et al. (2002) AKT proto-oncogene overexpression is an early event during sporadic colon carcinogenesis. Carcinogenesis 23: 201–205. PMID: 11756242

150. Rychahou PG, Kang J, Gulhati P, Doan HQ, Chen LA, et al. (2008) Akt2 overexpression plays a critical role in the establishment of colorectal cancer metastasis. Proc Natl Acad Sci U S A 105: 20315–20320. doi: 10.1073/pnas.0810715105 PMID: 19075230

151. Steinway SN, Gomez Tejeda Zañudo J, Ding W, Rountree CB, Feith DJ, et al. (2014) Network modeling of TGFβ signaling in hepatocellular carcinoma epithelial-to-mesenchymal transition reveals joint Sonic hedgehog and Wnt pathway activation. Cancer Res. doi: 10.1158/0008-5472.CAN-14-0225

152. Nakabayashi H, Taketa K, Miyano K, Yamane T, Sato J (1982) Growth of human hepatoma cells lines with differentiated functions in chemically defined medium. Cancer Res 42: 3858–3863. PMID: 6286115

153. Alexander JJ, Bey EM, Geddes EW, Lecatsas G (1976) Establishment of a continuously growing cell line from primary carcinoma of the liver. S Afr Med J 50: 2124–2128. PMID: 63998

154. Lin Y, Shi CY, Li B, Soo BH, Mohammed-Ali S, et al. (1996) Tumour suppressor p53 and Rb genes in human hepatocellular carcinoma. Ann Acad Med Singapore 25: 22–30. PMID: 8779541

155. Austinat M, Dunsch R, Wittekind C, Tannapfel A, Gebhardt R, et al. (2008) Correlation between beta-catenin mutations and expression of Wnt-signaling target genes in hepatocellular carcinoma. Mol Cancer 7: 21. doi: 10.1186/1476-4598-7-21 PMID: 18282277